

POLITECNICO DI TORINO

Master's Degree in Mechanical Engineering



Master's Degree Thesis

ESTIMATION OF THE PERFORMANCE OF A DESALINATION
SYSTEM BASED ON SORPTION PHENOMENA DRIVEN BY
SOLAR THERMAL ENERGY

Supervisors

Prof. Matteo Fasano

Prof. Eliodoro Chiavazzo

Co-supervisor

Dr. Matteo Morciano

Candidate

Maria Eliana Recchia

Academic Year 2020/2021

To my family

Contents

Contents	i
List of Figures	iii
List of Tables	viii
Abstract	1
1 Introduction	2
1.1 Desalination, thermochemical storage and co-generation	5
1.1.1 Desalination	6
1.1.2 Thermochemical storage	6
1.1.3 Co-generation	8
1.2 A focus on the components and the working principle of an adsorbed based desalination (AD) system	9
1.3 Adsorption working pairs	13
1.3.1 Adsorbent	13
Silica gel	14
Zeolite	14
1.3.2 Refrigerant	16
1.4 Evacuated solar panels	17
1.5 Previous studies	17
2 Numerical Model and Methods	20
2.1 AD system considered	20
2.2 Model details	21
2.2.1 Model assumptions	22
2.2.2 Mathematical Modeling	24
Adsorption equilibrium and Mass transfer	24

Heat transfer	26
Coefficient of performance	27
Initial and boundary conditions	28
2.3 Tools and solution methodology	29
3 Results	34
3.1 Heat flux influence on the system performance	34
3.2 Evaporation temperature influence on the system performance	39
3.3 Temperature distribution and Temperature profile	43
4 Discussion and Conclusion	49
4.1 Future development	50
5 Appendix	52
5.1 Variation of the Heat Flux at different pressures of the system	52
5.1.1 $T_{evap} = 20^{\circ}\text{C}$ and $P = 1100$ Pa	52
5.1.2 $T_{evap} = 20^{\circ}\text{C}$ and $P = 1200$ Pa	54
5.1.3 $T_{evap} = 20^{\circ}\text{C}$ and $P = 1300$ Pa	56
5.1.4 $T_{evap} = 20^{\circ}\text{C}$ and $P = 1400$ Pa	58
5.2 Variation of the evaporation temperature at different pressures of the system	60
5.2.1 $Heat\ Flux = 500\ \text{W/m}^2$ and $P = 1100$ Pa	60
5.2.2 $Heat\ Flux = 500\ \text{W/m}^2$ and $P = 1200$ Pa	62
5.2.3 $Heat\ Flux = 500\ \text{W/m}^2$ and $P = 1300$ Pa	64
5.2.4 $Heat\ Flux = 500\ \text{W/m}^2$ and $P = 1400$ Pa	66
5.2.5 $Heat\ Flux = 500\ \text{W/m}^2$ and $P = 1500$ Pa	68
Acknowledgements	72
References	73

List of Figures

1.1	Area of physical and economic water scarcity. Picture taken from <i>IWMI report, Insights from the Comprehensive Assessment of Water Management in Agriculture, Stockholm World Water Week, 2006 (Ref. [44])</i> . . .	3
1.2	A prediction of global water scarcity in 2025; <i>Source: International Water Management Institute website</i>	5
1.3	Advantages and disadvantages of desalination techniques, Picture taken from <i>Water desalination – Tap into the liquid Gold, (Ref. [15]), Sources: European Desalination Society (www.edsoc.com), International Desalination Association (www.idadesal.org), Universities Council on Water Resources (www.ucowr.siu.edu)</i>	7
1.4	Thermochemical energy storage: adsorption and desorption processes, Picture taken from <i>R. Bubbico, B. Mazzarotta, C. Menale, 2016 (Ref. [49])</i>	8
1.5	Schematic of a two-bed AD system. Picture taken from <i>Wu, Biggs, Hu, 2014, (Ref. [1])</i>	11
1.6	P-T-X working principle diagram of an AD cycle. Picture taken from <i>Wu, Biggs, Hu, 2014 (Ref. [1])</i>	13
1.7	Zoom on SiO ₄ in silica gel. Picture taken from <i>L.W. Wang, R.Z. Wang, R.G. Oliveira, 2009 (Ref. [9])</i>	15
1.8	Crystal cell unit of zeolite: (a) crystal cell unit of type A zeolite; (b) crystal cell unit of type X, Y zeolite. Picture taken from <i>L.W. Wang, R.Z. Wang, R.G. Oliveira, 2009 (Ref. [9])</i>	16
1.9	Schematic diagram of an adsorption desalination system. Picture taken from <i>Raj, Baiju, 2019 (Ref. [18])</i>	18
2.1	Schematic plant of the major components of the system	21
2.2	The prototypical single-bed adsorption-based desalination system considered here. Picture taken from <i>Wu, Biggs, Hu, 2014 (Ref. [1])</i>	22

2.3	The cross-section of adsorbent bed considered here. Picture taken from <i>Wu, Biggs, Hu, 2014 (Ref. [1])</i>	24
2.4	Hollow cylindrical thermal object, representing the core of the system, cell labels on	30
2.5	Hollow cylindrical thermal object, representing the core of the system, edge labels on	31
2.6	Mesh with triangular elements, 3-D problem	31
2.7	Mesh with triangular elements, 2-D problem	32
2.8	Simulink layout for solving the adsorption equations	32
3.1	Mass of water generated in a single cycle from one bed, as a function of the Heat Flux	35
3.2	Total heating and cooling requirement of a single cycle, as a function of the Heat Flux	36
3.3	Coefficient of performance of the process, as a function of the Heat Flux	36
3.4	Coefficient of performance of the process as a function of the water production	37
3.5	Coefficient of performance at final time (3000 s), for different pressures and heat fluxes, $T_{\text{evap}} = 20^{\circ}\text{C}$	38
3.6	Mass of fresh water generated at final time (3000 s), for different pressures and heat fluxes, $T_{\text{evap}} = 20^{\circ}\text{C}$	38
3.7	Mass of water generated in a single cycle from one bed, as a function of the evaporator temperature	39
3.8	Total heating and cooling requirement of a single cycle, as a function of the evaporator temperature	40
3.9	Coefficient of performance of the process, as a function of the evaporator temperature	40
3.10	Coefficient of performance of the process as a function of the water production	41
3.11	Coefficient of performance of the process as a function of the water production, zoom of Fig. 3.10	41
3.12	Coefficient of performance at final time (3000 s), for different pressures and evaporation temperature, Heat Flux = 500 W/m^2	43
3.13	Mass of fresh water generated at final time (3000 s), for different pressures and evaporation temperature, Heat Flux = 500 W/m^2	43

3.14	Temperature distribution for different heat fluxes: (a) 500 W/m ² , (b) 600 W/m ² , (c) 700 W/m ² , (d) 800 W/m ² , (e) 900 W/m ² , (f) 1000 W/m ²	44
3.15	Temperature distribution for different evaporation temperatures: (a) 5 °C, (b) 10 °C, (c) 15 °C, (d) 20 °C, (e) 25 °C, (f) 30 °C, (g) 35 °C, (h) 40 °C	45
3.16	An example of one of the temperature profile at different radius value . .	46
3.17	Evolution of the maximum temperature, reached on the external core surface (outer radius), at final time (3000 s) for a fixed heat flux (500 W/m ²), varying evaporation temperature and pressure of the system . .	47
3.18	Evolution of the maximum temperature, reached on the external core surface (outer radius), at final time (3000 s) for a fixed evaporation temperature (20 °C), varying heat flux and pressure of the system	48
5.1	Mass of water generated in a single cycle from one bed, as a function of the Heat Flux, P=1100 Pa	52
5.2	Total heating and cooling requirement of a single cycle, as a function of the Heat Flux, P=1100 Pa	53
5.3	Coefficient of performance of the process, as a function of the Heat Flux, P=1100 Pa	53
5.4	Coefficient of performance of the process as a function of the water production, P=1100 Pa	54
5.5	Mass of water generated in a single cycle from one bed, as a function of the Heat Flux, P=1200 Pa	54
5.6	Total heating and cooling requirement of a single cycle, as a function of the Heat Flux, P=1200 Pa	55
5.7	Coefficient of performance of the process, as a function of the Heat Flux, P=1200 Pa	55
5.8	Coefficient of performance of the process as a function of the water production, P=1200 Pa	56
5.9	Mass of water generated in a single cycle from one bed, as a function of the Heat Flux, P=1300 Pa	56
5.10	Total heating and cooling requirement of a single cycle, as a function of the Heat Flux, P=1300 Pa	57
5.11	Coefficient of performance of the process, as a function of the Heat Flux, P=1300 Pa	57

5.12	Coefficient of performance of the process as a function of the water production, $P=1300$ Pa	58
5.13	Mass of water generated in a single cycle from one bed, as a function of the Heat Flux, $P=1400$ Pa	58
5.14	Total heating and cooling requirement of a single cycle, as a function of the Heat Flux, $P=1400$ Pa	59
5.15	Coefficient of performance of the process, as a function of the Heat Flux, $P=1400$ Pa	59
5.16	Coefficient of performance of the process as a function of the water production, $P=1400$ Pa	60
5.17	Mass of water generated in a single cycle from one bed, as a function of the evaporation temperature, $P=1100$ Pa	60
5.18	Total heating and cooling requirement of a single cycle, as a function of the evaporation temperature, $P=1100$ Pa	61
5.19	Coefficient of performance of the process, as a function of the evaporation temperature, $P=1100$ Pa	61
5.20	Coefficient of performance of the process as a function of the water production, $P=1100$ Pa	62
5.21	Mass of water generated in a single cycle from one bed, as a function of the evaporation temperature, $P=1200$ Pa	62
5.22	Total heating and cooling requirement of a single cycle, as a function of the evaporation temperature, $P=1200$ Pa	63
5.23	Coefficient of performance of the process, as a function of the evaporation temperature, $P=1200$ Pa	63
5.24	Coefficient of performance of the process as a function of the water production, $P=1200$ Pa	64
5.25	Mass of water generated in a single cycle from one bed, as a function of the evaporation temperature, $P=1300$ Pa	64
5.26	Total heating and cooling requirement of a single cycle, as a function of the evaporation temperature, $P=1300$ Pa	65
5.27	Coefficient of performance of the process, as a function of the evaporation temperature, $P=1300$ Pa	65
5.28	Coefficient of performance of the process as a function of the water production, $P=1300$ Pa	66

5.29	Mass of water generated in a single cycle from one bed, as a function of the evaporation temperature, $P=1400$ Pa	66
5.30	Total heating and cooling requirement of a single cycle, as a function of the evaporation temperature, $P=1400$ Pa	67
5.31	Coefficient of performance of the process, as a function of the evaporation temperature, $P=1400$ Pa	67
5.32	Coefficient of performance of the process as a function of the water production, $P=1400$ Pa	68
5.33	Mass of water generated in a single cycle from one bed, as a function of the evaporation temperature, $P=1500$ Pa	68
5.34	Total heating and cooling requirement of a single cycle, as a function of the evaporation temperature, $P=1500$ Pa	69
5.35	Coefficient of performance of the process, as a function of the evaporation temperature, $P=1500$ Pa	69
5.36	Coefficient of performance of the process as a function of the water production, $P=1500$ Pa	70

List of Tables

2.1	Model parameters	33
3.1	Coefficient of performance, including the cooling effect at the evaporator, at final time (3000 s) for a fixed evaporation temperature (20 °C), varying heat flux and pressure of the system	37
3.2	Mass of fresh water generated, at final time (3000 s) for a fixed evaporation temperature (20 °C), varying heat flux and pressure of the system	37
3.3	Coefficient of performance, including the cooling effect at the evaporator, at final time (3000 s) for a fixed heat flux (500 W/m ²), varying evaporation temperature and pressure of the system	42
3.4	Mass of fresh water generated, at final time (3000 s), for a fixed heat flux (500 W/m ²), varying evaporation temperature and pressure of the system	42
3.5	Maximum temperature, reached on the external core surface, at final time (3000 s) for a fixed heat flux (500 W/m ²), varying evaporation temperature and pressure of the system	46
3.6	Maximum temperature, reached on the external core surface, at final time (3000 s) for a fixed evaporation temperature (20 °C), varying heat flux and pressure of the system	47

Abstract

Nowadays, adsorption desalination is one of the most attractive methods to obtain fresh and potable water, especially because it is environmental-friendly and economically, compared to the other desalting systems. In this thesis work, a desalination system based on sorption phenomena driven by solar thermal energy is investigated, in order to evaluate its performance and how to optimize them. The study of the plant under examination is divided into three macro-blocks: the first one is based on the solar technology; the second one is the environment-block that is focused on the evaporation temperature evaluation; the last one includes the major components such as the adsorbent bed, the evaporator and the condenser. Hence, a thermal and mass transfer numerical and mathematical model has been carried out. The purposes of producing distilled water, having a thermochemical storage and, finally, obtaining a cooling effect (similar to a heat pump able to set off a water purification treatment) can be reached simultaneously. The performance of the cycle have been calculated basically in terms of mass of fresh water generated after the desorption process and coefficient of performance, including the cooling effect at the evaporator. Subsequently, the results have been finally discussed.

Chapter 1

Introduction

Nowadays global demand for potable water is growing, due to agriculture, industrial and domestic sectors and it is already higher than the sustainable level. It is common knowledge that water is the most vital commodity and one of the most abundant resources of the earth. About 97% of water that covers the earth's surface is saline and only 3% is fresh water. Of this fraction, about 0,5% is suitable for human needs because the remaining portion is in the form of polar ice caps, glaciers and atmosphere.

For many different reasons, regions once rich in water resources find it difficult to meet the increasing demand. In line with this, rising water scarcity, that is becoming a serious phenomenon, is most severe, especially in semi-arid and desert regions and in countries with high population density or specialised in economic activities. Indeed, the increasing gap between demand and supply can be related to inadequate physical resources but also to the economical lack of techniques that make it possible to obtain fresh and potable water. Figure 1.1 highlights the global background.

Even if it is neither easy nor affordable, lots of engineering challenges aim to seek sustainable water supply alternatives. To better understand why, it might be useful to discuss the water quality and scarcity in drought areas. To make up an exhaustive and brief list of the main causes of water scarcity, first of all one can consider climate change, drought or low precipitations events, forest fires and floods. Secondly, another important factor is the overuse of water due to population growth, urbanization and economic development; this excessive use is also related to high living standards (electronic devices or luxurious tourism). Furthermore, environmental pollution, that involves, for example, domestic sewage, effluents originating from agriculture, animal feed operations, illegal discharges of wastewater or pollu-

tants from different activities, contributes to increase this critical phenomenon.

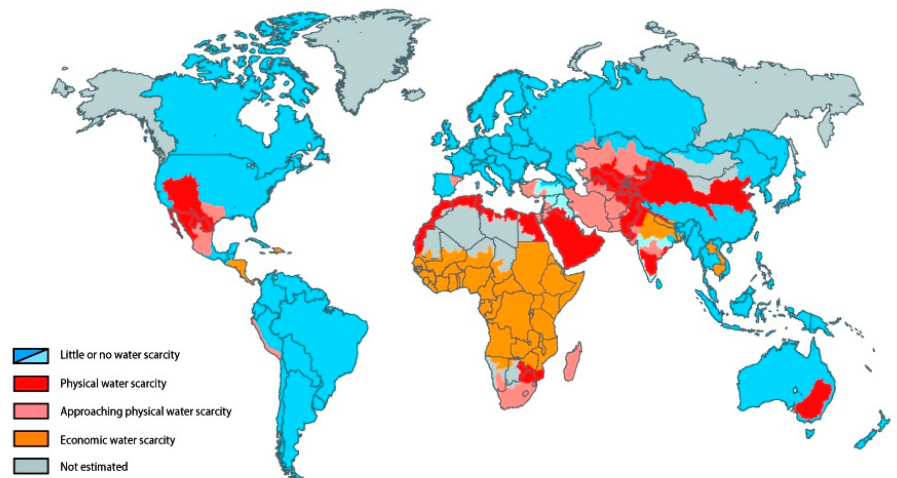


Figure 1.1: Area of physical and economic water scarcity. Picture taken from *IWMI report, Insights from the Comprehensive Assessment of Water Management in Agriculture, Stockholm World Water Week, 2006 (Ref. [44])*

Additionally, as reported by the International Water Management Institute (IWMI), Figure 1.2 shows a projection of World's water scarcity in 2025; in this perspective, implementing desalination technologies is a reasonable choice among the various possible and realizable solutions to mitigate the effects of water shortages.

Over the last few years, different desalination methods, defined as separation of salt and minerals from seawater molecules, have been developed as a practical solution to overcome this problem.

The major current traditional desalination processes in the World are:

- *Membrane Distillation (MD)*: a thermal membrane separation process, in which water vapour molecules and volatile compounds are transferred from saline water through a microporous hydrophobic membrane because of the partial pressure difference created by the temperature difference on both sides of the membrane;
- *Multistage Flash Distillation (MSFD)*: a thermal process carried out in a series of closed tanks, set at progressively lower pressures; when preheated seawater enters the first stage, some of it rapidly boils, forming vapour that is condensed into fresh water on heat-exchange tubes. So, fresh water is collected in tanks

and the remaining seawater flows into the next stage, where it flashes and the process is continued;

- *Multieffect Distillation (MED)*: a technique in which the liquid simply passed from a container under high atmospheric pressure to one under lower pressure; so, the reduced pressure causes the rapid liquid vaporization and the resulting vapour is then condensed into distillate;
- *Crystallization*: a method that utilizes the phase change of water from liquid to solid; it is based on the separation of the ice crystals from the brine, in order to remove any salts on the crystals surface, then ice melts to get lastly fresh water;
- *Mechanical Vapour Compression (MVC)*: a process where the feed, after passing through a heat exchanger, is converted to vapour and then compressed by mechanical means. The compressed vapour, as fresh water, has high temperature and pressure and is circulated through the initial heat exchanger to heat the incoming feed;
- *Electrodialysis*: a membrane process which uses an high electrical potential energy to separate cations and anions from the stream; this electrical potential forces the salt particles to move through a membrane, leaving behind fresh water as a product;
- *Reverse Osmosis (RO)*: a process based on the forced passage of water through a membrane against the natural osmotic pressure to separate water and ions. In these high pressures, the water molecules can pass through the membranes and the salts are left behind as a briny concentrate.

However, these methods are energy intensive, not environmental-friendly and have a number of other drawbacks, including high maintenance costs arising from fouling, corrosion, salt deposition and high working temperatures.

With this in mind, the aim is to seek an alternative and novel desalting system that ensures to obtain a significant amount of fresh water on one side and to consume less chemicals, thermal energy and electricity on the other.

One solution to this issue is the Adsorption-based desalination (AD) that, compared with the conventional techniques, has several advantages:

- Reduction of fouling and corrosion, as the result of the low operating temperatures and the confinement of saline water in a fraction of the total system;
- Reduction in maintenance costs, due to fewer moving parts;
- Double distillation;
- Possibility to treat or desalinate waters containing organic compounds;
- Two useful effects: co-generate potable water and cooling (using waste heat or renewable energy).

Projected Global Water Scarcity, 2025

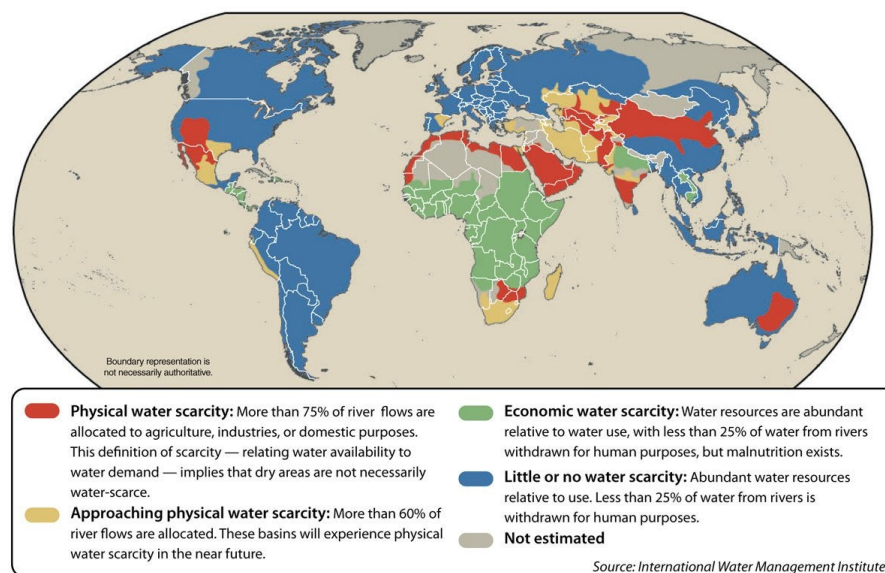


Figure 1.2: A prediction of global water scarcity in 2025; *Source: International Water Management Institute website*

1.1 Desalination, thermochemical storage and co-generation

In this thesis, three remarkable key words are desalination, thermochemical storage and co-generation.

1.1.1 Desalination

Water desalination is the process of separating the salts from a saline solution, for example brackish water or seawater, in order to obtain water suitable for industrial or agricultural uses and for human consumption.

The process of desalination takes place in desalination plants. It involves different phases: the first one is the collection of brackish water; secondly, with a pre-treatment, physical, chemical and biological properties of the water are modified and suited for the treatment in the desalination plant; then, the main phase is the desalination itself, that occurs using one of the available techniques like distillation, evaporation or membranes processes. Finally, the desalinated water in output is post-treated with the purpose of correcting its hardness and low alkalinity.

Most of the modern interest in desalination is focused on developing affordable ways of providing fresh water for human use, especially in regions where the availability of water is limited. Large-scale desalination often requires large amounts of energy, specialized and expensive infrastructure, making it very costly compared to the use of fresh water from rivers or groundwater. Keeping in mind the overview of the most common desalination techniques listed at the beginning of this chapter, the following table (Figure 1.3) could be a good way to summarize what has been said so far.

1.1.2 Thermochemical storage

Overall, thermal energy storages are based on the internal energy variation (in the form of latent heat, sensible heat or thermochemical energy) of a specified material. From a properly energetic point of view, in a thermal energy storage there are the following phases.

1. Charging phase: heat is transferred to the storage (containing a liquid or solid material) in a fixed time range;
2. Storing phase: heat is stored as thermal energy, in the form of cool or warm;
3. Discharging phase: the previous energy is released when is required.

An example is the thermal energy storage with renewable energies, as the solar one used in the plant here presented. In fact, due to the storage capacity, the flux coming from the solar panels is available in a continuous manner, also during

Desalination type	Usage	Advantages	Disadvantages	Companies
Distillation				
Multi-stage flash distillation (MSF) Desalination process that distills seawater by flashing a portion of the water into steam in multiple stages of what are essentially regenerative heat exchangers.	Accounts for 85% of all desalinated water, used since early 1950s	MSF plants, especially large ones, produce a lot of waste heat and can therefore often be paired with cogeneration	High operating costs when waste heat is not available for distillation. High rates of corrosion	Doosan Heavy Industries (South Korea)
Multiple-effect evaporator (MED/ME) Using the heat from steam to evaporate water. In a multiple-effect evaporator, water is boiled in a sequence of vessels, each held at a lower pressure than the last.	Widely used, since 1845	High efficiency, while relatively inexpensive	A large heating area is required	Niro (United States)
Vapor-compression evaporation (VC) Evaporation method by which a blower, compressor or jet ejector is used to compress, and thus, increase the temperature of the vapor produced.	Mainly used for wastewater recovery	Technique copes well with high salt content in water	-	Vacom, Water Desalination International (United States)
Evaporation/condensation Evaporation of seawater or brackish water and consecutive condensation of the generated humid air, mostly at ambient pressure.	Widely used	Easiest method of distillation	Time-consuming and inefficient in comparison to other techniques	-
Membrane processes				
Electrodialysis reversal (EDR) Electrochemical separation process that removes ions and other charged species from water and other fluids.	Widely used, since early 1960s	Long membrane lifetime and high efficiency (up to 94% water recovery, usually around 80%)	High capital and operational costs	General Electric (GE), Ryan Heroo Flow Solutions (United States)
Reverse osmosis (RO) Separation process that uses pressure to force a solvent through a membrane that retains the solute on one side and allows the pure solvent to pass to the other side.	Widely used, first plant installed in Saudi Arabia in 1979	In water purification, effectively removes all types of contaminants to some extent	Requires more pretreatment of the seawater and more maintenance than MSF plants	Multiplex-Degremont Joint Venture (Australia) Consolidation Water (Cayman Islands), GE
Nanofiltration (NF) Nanofiltration membranes have a pore size in the order of nanometers and are increasingly being used for water desalination.	Emerging technology	Very high efficiency	High capital cost, unknown lifetime of membrane, no large-scale plant built yet	Stoneybrook Purification (United States)
Forward osmosis (FO) Osmotic process that, like reverse osmosis, uses a semi-permeable membrane to effect separation of water from dissolved solutes.	Emerging technology	Low or no hydraulic pressures, no energy needed for separation	Cannot produce pure water, only concentrated solutions	Apaciara (United Kingdom)
Membrane distillation (MD) In membrane distillation, the driving force for desalination is the difference in vapor pressure of water across the membrane, rather than total pressure.	Widely used	Low energy consumption, low fouling	-	KeppelSeghers (Belgium)

Figure 1.3: Advantages and disadvantages of desalination techniques, Picture taken from *Water desalination – Tap into the liquid Gold*, (Ref. [15]), Sources: *European Desalination Society* (www.edsoc.com), *International Desalination Association* (www.idadesal.org), *Universities Council on Water Resources* (www.ucowr.siu.edu)

night hours. In particular, dealing with thermochemical energy storages, it has a relevant role the energy absorbed and released for the break and link of the chemical bonds (bond reactions) of the material into the vessel. Here the surplus chemical energy is transformed in heat and vice versa, depending on whether energy itself is requested by users or it must be stocked. Taking this thesis work into account, the adsorption process (silica gel – water or zeolite – water pairs) can be seen as a great way to stock cool or warm. Figure 1.4 (*R. Bubbico, B. Mazzarotta, C. Menale, Settembre 2016*) depicts the thermochemical storage connected with the adsorption and desorption processes. During the charging period, water is desorbed by the inner surface of adsorbent and then there is a period of transition, which represents

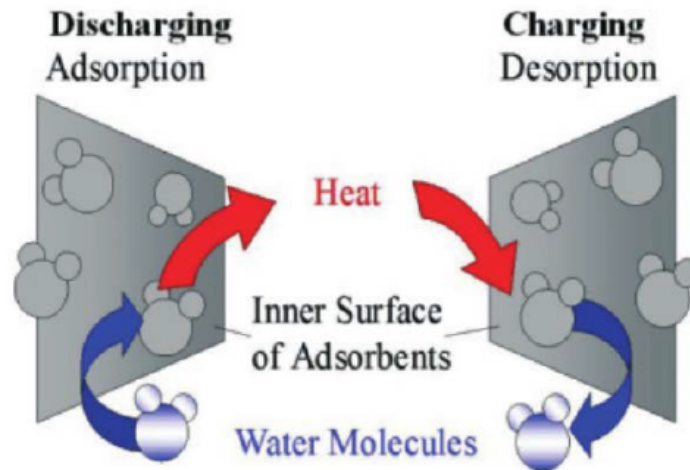


Figure 1.4: Thermochemical energy storage: adsorption and desorption processes, Picture taken from *R. Bubbico, B. Mazzarotta, C. Menale, 2016 (Ref. [49])*

the storing phase; subsequently, when the adsorbent bed adsorbs water molecules, the discharging period starts and so on.

1.1.3 Co-generation

Co-generation, also known as combined heat and power (CHP), is defined as the sequential generation of two different forms of useful energy from a single primary energy source, typically mechanical energy or thermal energy. Mechanical energy may be used either to drive an alternator for producing electricity or rotating equipment such as motor, compressor, pump or to drive a fan, useful for providing different services. Thermal energy, indeed, may be used either for direct process applications or for the indirect production of steam, hot water, chilled water for process cooling or hot air for dryer.

Co-generation seems to have significant long-term prospects in global energy markets due to its numerous environmental and economic benefits:

- Reduction in energy use affordably and improvement in security of energy supply;
- Electrical grid losses reduction, when co-generation plants are located close to consumers; in addition, co-generation is often well suited for use in isolated or remote areas;

- Heat losses, that are one of the main drawbacks of conventional electrical systems, are reduced and efficiency is increased when co-generation is used to supply heat to various applications and facilities, listed below;
- Co-generation can offer an attractive option for facilities with high electric rates and buildings that consume large amounts of hot water and electricity;
- Co-generation provides a wide range of technologies for application in various areas of economic activities; in fact, the thermal energy product from co-generation can be used for domestic hot water heating, space heating, pool and spa heating, laundry processes or absorption cooling. Moreover, facilities that use large amounts of thermal energy during all months of the year are apartments, condominiums, schools, universities, other educational institutions, hospitals, hotels, athletic clubs, assisted living facilities, nursing homes, industrial and waste treatment facilities.

The overall efficiency of energy use in co-generation mode, defined as the percent of the fuel converted to both electricity and useful thermal energy, is about 65% and it can be up to 85% and above in some cases.

Moreover, co-generation is often associated with the combustion of fossil fuels but it is interesting to highlight that it can also be carried out using other sources of thermal energy, such as renewable energy resources, nuclear energy and burning wastes. Recently the trend is to use cleaner fuels like natural gas for co-generation. Additionally, as well as the saving of fossil fuels, co-generation also allows to reduce the emission of greenhouse gases, particularly CO₂ emission.

1.2 A focus on the components and the working principle of an adsorbed based desalination (AD) system

It has long been known that a porous solid can take up relatively large volumes of vapours until the equilibrium conditions are achieved. This process is a spontaneous exothermic phenomenon called *adsorption*; in particular, the vapour adsorbed on the surface and the solid surface on which vapour is accumulated are called adsorbate

and adsorbent respectively. Adsorption of a gas by a solid is accompanied by the release of heat, called heat of adsorption, whereas the reverse process, defined as *desorption*, is an endothermic one. The performance of adsorption energy storage systems depend principally on the availability of the optimal and most appropriate adsorbent – adsorbate pair and, as a consequence, on its adsorption capacity, heat of adsorption, thermal stability and reactivation ability with the available energy sources.

In AD cycles, the principle of adsorption-desorption, by the adsorbent-adsorbate pair, is applied for the evaporation of the saline water and condensation of the vapour at lower temperatures, typically between 5 °C and 45 °C. Briefly, the saline solution evaporates and then the water vapour is adsorbed on the pore surfaces, due to the high vapour affinity of the adsorbent.

The most basic model of any practicable production system, capable of producing fresh water in an essentially continuous manner, is a two-bed adsorption-based desalinator. Generally speaking, the major components of this kind of system are: two (or more) adsorber/desorber beds, an evaporator-condenser device, a seawater tank and a potable water collection tank. The beds contain adsorbent materials (for example silica gel or zeolite or anyway hydrophilic and highly porous materials with huge surface area) and constitute the plant’s reactor or core; this could communicate with the evaporator or the condenser during the half-cycle periods via a series of dedicated valves. Figure 1.5 (*Wu, Biggs, Hu, 2014*) shows a schematic of a two-bed adsorption-based desalinator.

First of all the whole system is degassed and the saline water is charged into the evaporator; the valve 1 is opened and the source water, at temperature T_{evap} , evaporates, travels as a vapour into the bed 1 and it is adsorbed on the silica gel (or zeolite); the heat generated during the adsorption is removed by cold water (at T_{cw}) circulating in the manifold of bed 1. Once bed 1 is saturated with vapour, valve 1 is closed and, at the same time, the water circulating in bed 1 is switched to hot water (at T_{hw}) and the pressure in bed 1 is increased.

At the condenser pressure, valve 2 is opened and the hot water circulating through bed 1 drives off the water adsorbed on the silica gel to the condenser; the silica gel in bed 1 is then regenerated and the water in the condenser forms pure water (at T_{cond}). Valve 2 is closed, cold water is circulated through bed 1 to reduce the pressure and then the cycle is ready to re-start.

Bed 1 and bed 2 are operated alternatively in the way described to produce fresh

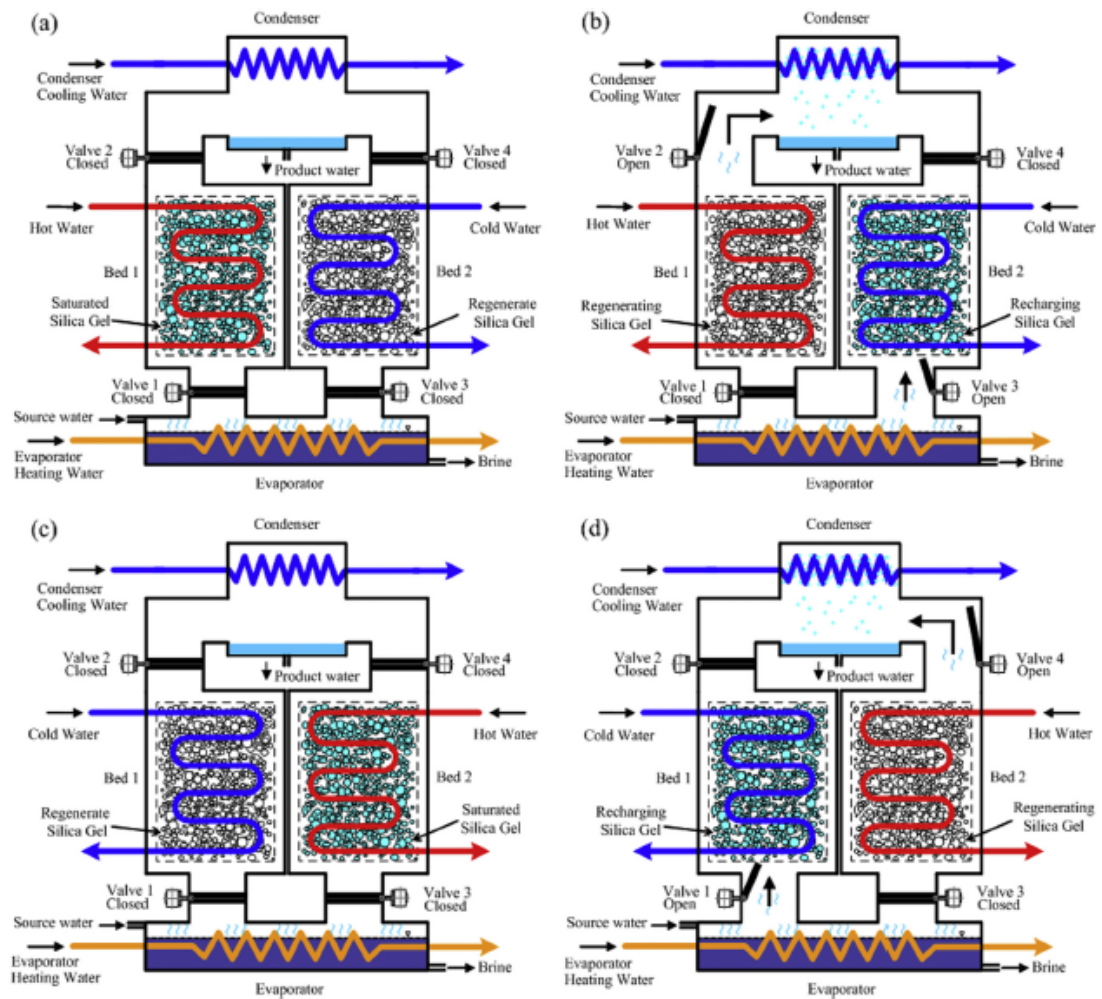


Figure 1.5: Schematic of a two-bed AD system. Picture taken from *Wu, Biggs, Hu, 2014, (Ref. [1])*

water in a continuous way.

Notice that in Figure 1.5:

- (a) Bed 1: Process from point 1 to point 2; Bed 2: Process from point 3 to point 4;
- (b) Bed 1: Process from point 2 to point 3; Bed 2: Process from point 4 to point 1;
- (c) Bed 1: Process from point 3 to point 4; Bed 2: Process from point 1 to point 2;
- (d) Bed 1: Process from point 4 to point 1; Bed 2: Process from point 2 to point 3.

Now, considering the cycle for one single bed and referring to the thermodynamic diagram in Figure 1.6 (*Wu, Biggs, Hu, 2014*), four different processes, two isosters and two isobars, can be outlined:

- Process 3 \rightarrow 4: ISOSTERIC COOLING

Assume the process starts at point 3: the silica gel (or zeolite) has its maximum temperature (T_{hw} about 80-90°C) and minimum rate of adsorbed water ($X_3 = X_{min}$). The bed is isolated from the evaporator and the condenser, the cold water starts to circulate through the bed so the silica gel (or zeolite) temperature decreases until point 4. At point 4, the bed temperature is about 60-70°C and its pressure is equal to the saturated pressure of pure water at T_{evap} . Valve 1, between bed and evaporator, is now opened.

- Process 4 \rightarrow 1: ISOBARIC COOLING/ADSORPTION

Once valve 1 is opened and cold water continues to circulate, saline water in the evaporator starts to evaporate: the vapour travels to the bed and the silica gel or zeolite bed adsorbs it. Pressure in bed and evaporator is constant (P_{evap}) and the temperature continues to decrease until point 1. At point 1, the bed temperature is equal to the temperature of the cold water circulating in the manifold through the bed (T_{cw}) while the amount of water adsorbed by the silica gel or zeolite is the maximum value possible ($X_1 = X_{max}$). Valve 1, between bed and evaporator is now closed.

- Process 1 \rightarrow 2: ISOSTERIC HEATING

Once valve 1 is closed, the cold water circulating through bed is switched to hot water to increase bed temperature and pressure. This process continues until point 2; at point 2 the pressure is equal to the saturation pressure of water at the condenser temperature (P_{cond}) and then valve 2, between bed and condenser, is opened.

- Process 2 \rightarrow 3: ISOBARIC HEATING/DESORPTION

Once valve 2 is opened, the vapour starts to be desorbed from the adsorbent bed and travels to the condenser, when it condenses. During this process, pressure in bed and condenser is constant and equal to P_{cond} until point 3; the amount of adsorbed water at the end of the process is equal to the minimum value X_3 . This process is the silica gel regeneration/ condensing process and fresh water production process.

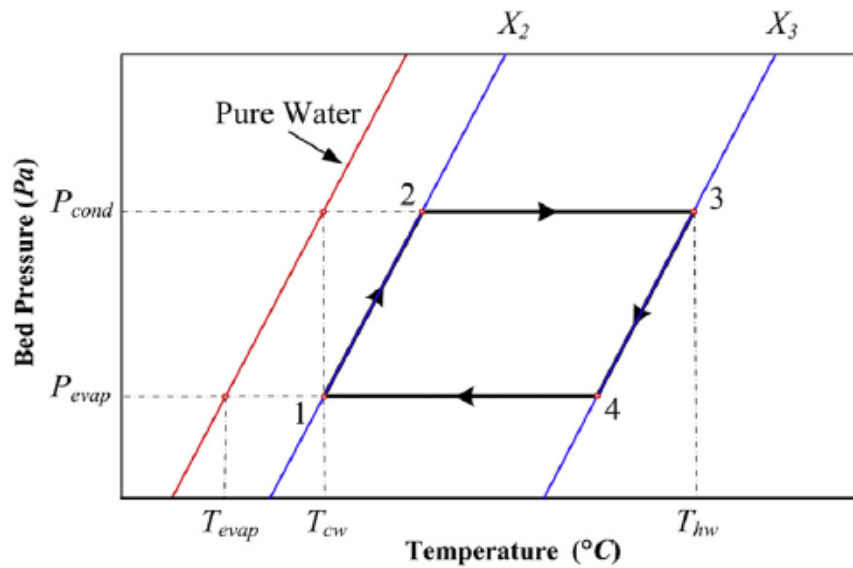


Figure 1.6: P-T-X working principle diagram of an AD cycle. Picture taken from *Wu, Biggs, Hu, 2014 (Ref. [1])*

It should be highlighted that the fresh water is distilled twice. At the same time, a cooling effect is generated at the evaporator, which can be used for air conditioning purposes, as in a normal adsorption chiller, or can be fed back to the bed or condenser. Moreover, the core works as a thermochemical storage. This means that an adsorption desalination system has the ability to perform as a chiller and double distilling desalinator simultaneously.

1.3 Adsorption working pairs

The choice of adsorbent-adsorbate combination is one of the significant problems in the investigation of AD systems. In particular, focusing on physical adsorption, this is caused by van der Waals forces and the electrostatic force between the molecules of the adsorbent and the surface atoms adsorbate. Physical adsorbents with mesopores can adsorb consecutive layers of adsorbate, the ones with micropores have the volume of the pores filled with the adsorbate.

1.3.1 Adsorbent

The common physical adsorbents used for this kind of systems are activated carbon, activated carbon fibre, silica gel and zeolite. In this thesis work, silica gel and zeolite have been compared.

Commercial adsorbents are porous solids with internal surface areas much greater than external ones, so their total surface areas are almost equal to their internal surface ones. Adsorbents are classified into three basic types according to their pore sizes:

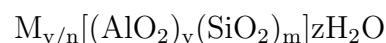
- Micropores (ultramicro-pore or supermicro-pore): pore size < 2 nm;
- Mesopores: pore size 2-50 nm;
- Macropores: pore size > 50 nm.

Silica gel

The silica gel is a type of amorphous synthetic silica. As shown in Figure 1.7 (*Wang L.W., Wang R.Z., Oliveira R.G., 2009*), it is a rigid, continuous net of colloidal silica, linked to very small grains of hydrated SiO_4 . The hydroxyl in the structure is the adsorption centre because it is polar and can form hydrogen bonds with polar oxides, such as water and alcohol. One hydroxyl can adsorb one molecule of water. Moreover, silica gel looks like irregular crystal, with an extremely high surface's area that makes it a perfect desiccant. It has very stable thermal and chemical characteristics, it is non-toxic, odorless, non-corrosive, non-flammable and it can absorb up to 40% of its own weight. Additionally, silica gel has low generation temperatures and it can be reused after a regeneration process; it can be conveniently packed and is available in a many sizes for various applications. Each kind of silica gel has only one type of pore; typically, the pore diameters are 2-3 nm (A type) and 0,7 nm (B type), while the specific surface area is about 100–1000 m^2/g . Type A silica gel could be used for all desiccation conditions, but type B silica gel can only be used when the relative humidity is higher than 50%.

Zeolite

Zeolite is a type of hydrated alumina silicate (of group I and group II elements) crystal composed of alkali or alkali soil. The chemical formula of zeolite is



where y and m are all integers and m/y is equal or larger than 1. n is the chemical valence of positive ion of M , z is the number of water molecules inside a crystal cell

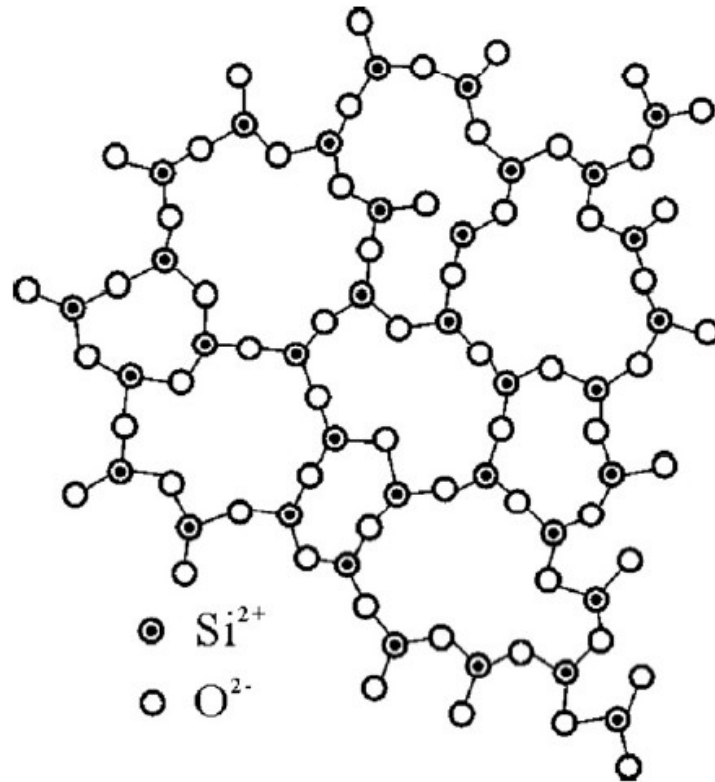


Figure 1.7: Zoom on SiO_4 in silica gel. Picture taken from *L.W. Wang, R.Z. Wang, R.G. Oliveira, 2009 (Ref. [9])*

unit.

A crystal cell unit of zeolite, that is very regular in its pore size, is shown in Figure 1.8 (*Wang L.W., Wang R.Z., Oliveira R.G., 2009*). The electric charge of the positive ion and the electric charge of aluminium atom must be balanced (note that the net electric charge of each aluminium atom is -1). The alumina silicate skeleton has a porosity between 0,2 and 0,5, is similar to a cage and it is usually connected by six sections, which can adsorb a large amount of extra molecules. Then, water eventually adsorbed can be removed by heating.

There are about 40 types of natural zeolites and the ones mainly utilized in adsorption applications are chabazite, sodium chabazite, cowlesite and faujasite. Furthermore, about 150 types of zeolites can be artificially synthesized and they are named by one letter or a group of letters, such as type A, X, Y, ZSM and so on. 4A, 5A, 10X and 13X zeolites are the main types used for adsorption system. Artificially synthesized zeolites are more expensive than natural zeolites but they have higher bulk specific weight and better heat transfer performance.

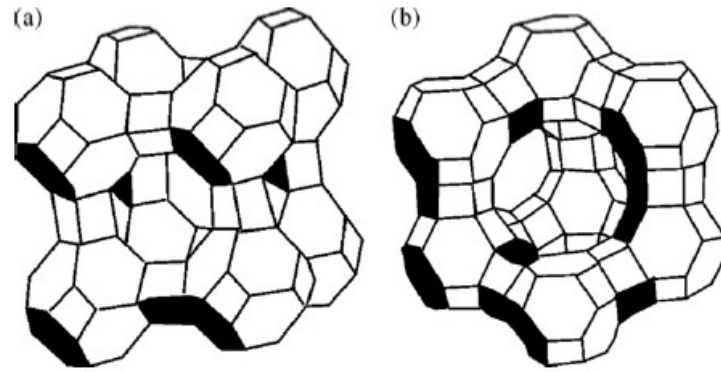


Figure 1.8: Crystal cell unit of zeolite: (a) crystal cell unit of type A zeolite; (b) crystal cell unit of type X, Y zeolite. Picture taken from *L.W. Wang, R.Z. Wang, R.G. Oliveira, 2009 (Ref. [9])*

The adsorption ability of zeolites is related to the proportion between Si and Al and the adsorption ability is higher, smaller this proportion is. The pore size of zeolites (0,3-1 nm) determines the selectivity for different adsorbates. Artificially synthesized zeolites have micropores with uniform size and different sizes can be obtained by different manufacturing methods. The adsorption and desorption heat of zeolite pairs and their desorption temperature are high; at the same time, most zeolites can be destructed at temperatures higher than 600–700 °C so they are usually employed in adsorption systems that have heat source between 200 and 300°C.

1.3.2 Refrigerant

The choice of the type of refrigerant depends on the different application (for example air conditioning, refrigeration or the upgrade of heat with thermal transformers). An optimal refrigerant should have high latent heat of vaporization per volume unit or mass unit, thermal stability, saturation pressure between 1 and 5 atm in the working temperatures and should be environmental harmless, non-flammable and innocuous; unfortunately, there are no refrigerants that have all the characteristics above concomitantly.

Focusing on this thesis topic, for adsorption system the common refrigerants are water, ammonia and methanol. Ammonia can be used with chlorides, activated carbon or activated carbon fibre while methanol is normally employed in pair with activated carbon or activated carbon fibre. Instead, water could be considered as a perfect refrigerant; even if it has an extreme low saturation pressure and it is not

able to produce temperatures below 0°C , water presents excellent physical and thermal properties such as high latent heat of evaporation, low viscosity, high thermal conductivity, thermal stability in a wide range of operating temperature and a compatibility with several materials. Due to all these advantages, water is typically used in association with silica gel or zeolite, so it is the kind of adsorbate here considered. Moreover, in order to complete the discussion, hydrogen and oxygen are examples of other refrigerants that can be adopted; in particular, hydrides are the adsorbents for hydrogen, that comes from the decomposition of water, but because of its inflammability and explosiveness, it requires extremely precaution to be handled. The types of oxygen that can be adsorbed by oxides are O_2 , O_2^- , O^- and O_2^+ . The reaction between oxides and oxygen has large enthalpy and for this reason, it is usually employed in chemical heat pumps, but it is also suitable for cryogenic system with temperatures below 120 K. Finally, other refrigerants, as R134a, R22, R407c and ethanol can be utilized with activated carbon or activated carbon fibre.

1.4 Evacuated solar panels

Keeping in mind what has been said above about the thermodynamic AD cycle and in particular that the adsorption continues until the silica gel saturated with water vapour and closing the valve between the adsorbent bed and evaporator, it is important to notice that, in this thesis project, during the desorption process, the saturated silica gel (or zeolite) is regenerated using hot water coming from a solar collector.

So, it is evident that the aim of this work is to analyze the performance of a solar powered adsorption cooling and desalination system. To better understand the major components of the system and, generally, what has been described until now, Figure 1.9 (*Raj, Baiju, 2019*) depicts an exhaustive and clear scheme of this kind of desalination plant.

1.5 Previous studies

As reported by Leong and Liu (2004) in their numerical model for an adsorption-cooling system based on the combination of heat and mass transfer, in recent years, many scientists have studied various layout of such systems. The aim was to investigate the parameters that have a great influence on the thermal performance and

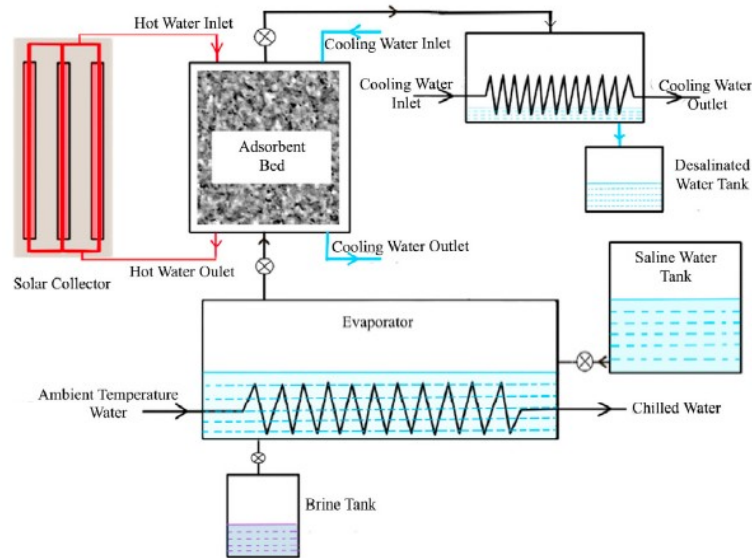


Figure 1.9: Schematic diagram of an adsorption desalination system. Picture taken from *Raj, Baiju, 2019 (Ref. [18])*

to understand how to improve the plants itself.

Many investigators have studied the increment of thermal conductivity of adsorbent bed; others have presented numerical studies to optimize heat and mass transfer properties of adsorption systems. In most of these numerical studies, it was assumed an adsorptive equilibrium and neglected the internal mass transfer resistance between the solid and the adsorbate gas; in fact, in actual systems, it was stated that the solid and the gas do not reach equilibrium instantly, so the internal resistance is effectively negligible only considering long cycle process times. Moreover, the performance can be significantly reduced because of internal mass transfer that can be described by a linear driven force model. Several papers have developed a one (or two) dimensional dynamic mathematical model of an AD system, describing the combined heat and mass transfer in adsorbent bed (including gas flow in adsorbent bed model, lineal force driven model and equivalent heat transfer conductivity of adsorbent bed model).

To study the thermal performance of the system (in terms of fresh water production rate, energy consumption, COP), many researchers investigated the effects of parameters such as the heat and mass transfer coefficients, thickness of the bed, diameter of the particles, porosity and so on; generally there are lumped AD models where transport phenomena are ignored or not modelled explicitly and models that include spatial gradients and related transport processes. So, one can find in liter-

ature 1-D, 2-D or 3-D models, which may or may not be experimentally-validated using simplified or more detailed approaches.

Chapter 2

Numerical Model and Methods

Considering what has been said in the Introduction about the working principle of an adsorption-based desalinator, now it is possible to draw up the prototypical single-bed AD system studied in this thesis work. It can be noticed that the plant described here is very similar to the one depicted in Figure 1.9 (*Raj, Baiju, 2019*) in the previous chapter.

2.1 AD system considered

First of all, here it is presented a method of desalination that has the ability to produce both potable water and cooling effect. In Figure 2.1 is represented a schematic plant of the major components of the system, that uses a low-grade heat from the solar collector to generate water vapour from the adsorber.

- *Evaporator*: saline water is charged in it and evaporates under low pressure; at the same time, chilled water is circulated in it, to maintain the evaporator process (notice that it can be used for chilling purposes);
- *Valve between the adsorbent bed and the evaporator*: when it is opened, water evaporates and travels into the bed; after the adsorption process, when silica gel saturated with water vapour, the valve is closed;
- *Thermochemical storage*: it is the plant's core, namely the adsorbent silica gel (or zeolite) bed; it adsorbs water coming from the evaporator;
- *Valve between adsorbent bed and condenser*: when it is opened, water generated from the desorption process travels into the condenser;

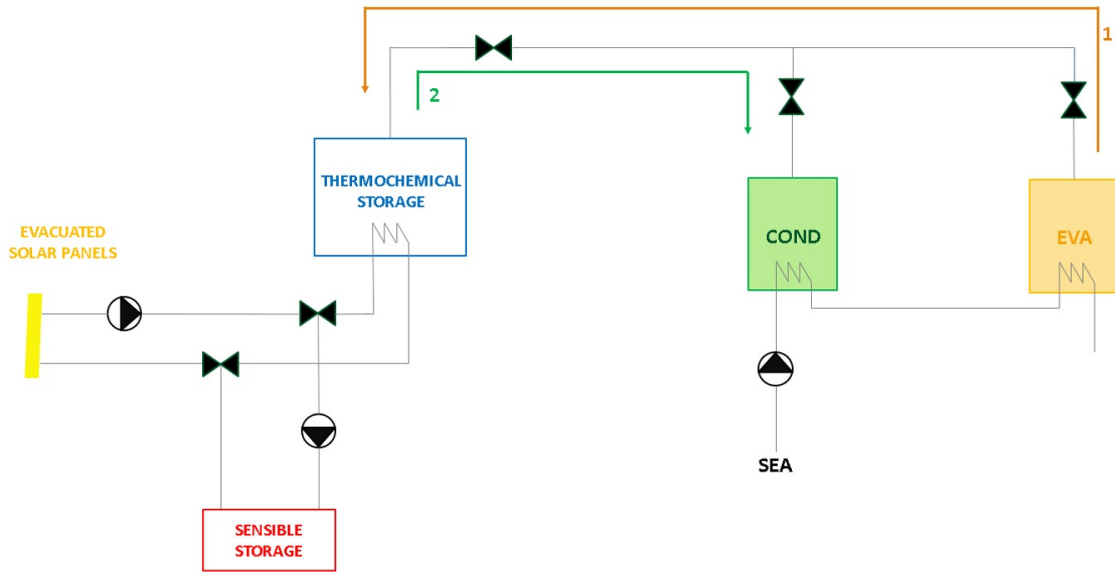


Figure 2.1: Schematic plant of the major components of the system

- *Sensible or latent storage*: it is located between the thermochemical storage and the solar panels and it may be useful when there is too much heat, which is not used in the thermochemical storage; so this surplus is stored as sensible heat;
- *Condenser*: cooling water is circulated through it and the condensate is collected as pure water; it can be highlight that in this plant, the condenser and the evaporator are not a single integrated device, but they are separated in order to obtain the co-generation effect;
- *Solar evacuated panels*: they are characterized by an heat flux, used to obtain hot water that regenerates the saturated silica gel and so to drive the desorption process;
- *Hydraulic pumps*: in this scheme, they are used to better understand the direction of water or steam.

2.2 Model details

The model of the adsorption-based desalination system developed here is basically a one single-bed AD system, very similar to the one shown in Figure 2.2 (*Wu, Biggs, Hu, 2014*). The core, also defined as the thermochemical storage, is of a hollow cylindrical shape, which is the most usual geometry used for this kind of application;

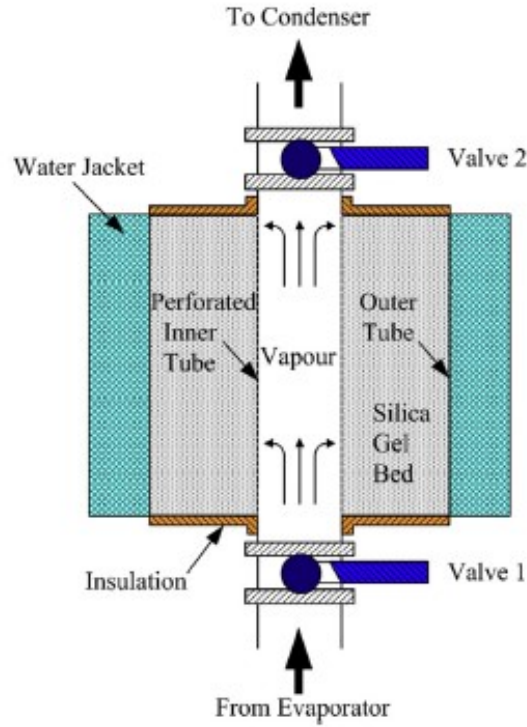


Figure 2.2: The prototypical single-bed adsorption-based desalination system considered here. Picture taken from *Wu, Biggs, Hu, 2014 (Ref. [1])*

a stainless-steel material is used for this device. Therefore, the adsorbent bed lies between a thin outer tube of radius r_o and a perforated inner pipe of radius r_i ; this one is connected to the evaporator or the condenser, alternatively, by the two valves already discussed. The bed is heated and cooled by a water jacket, located around the outer tube, receiving the heat flux from the evacuated solar panels.

2.2.1 Model assumptions

The mathematical model drawn up in this thesis follows the hypothesis below. It should be pointed out that the numerical study carried out is not be experimentally-validated yet.

The assumptions are:

1. The vapour phase is an ideal gas, so its properties can be evaluated using the Ideal Gas Law;
2. The adsorbent bed is composed of uniformly-sized particles and has isotropic properties;

3. Mass flow is assumed to occur in the radial direction only because of resistance to flow through the bed is much greater than along the inner tube; so mass transfer in the axial and circumferential direction of the bed is negligible;
4. Similarly, heat transfer in the axial and circumferential direction of the bed is negligible, because the ends of the cylinder are well insulated and heat transfer can only occur in radial direction;
5. Mass transfer from the vapour phase into the particle is described by a linear driving force model;
6. The thermal resistance between the vapour phase and the bed particles is small, so the local temperature of steam and silica gel is supposed to be the same;
7. At the same time, the thermal resistance between the outer metal wall of the cylinder and the water jacket is small, so it is assumed that the wall temperature is equal to the temperature of the water circulating through the water jacket;
8. During the cooling and heating bed processes, the water jacket temperature is constant;
9. The heat transfer between the system and the water jacket is the only one not negligible;
10. Heat losses from the adsorbent bed, the evaporator and the condenser are neglected;
11. The adsorption isotherms are assumed to be equal to the desorption ones;
12. The properties of all solid materials are temperature independent.

As a result of these observations, particularly of point 3 and 4, to study the transport phenomena, in order to reduce the computational cost, the core of the system is considered as a circular annulus with an infinitesimally small height, rather than a cylinder. Figure 2.3 (*Wu, Biggs, Hu, 2014*) shows a cross-section of the adsorbent bed.

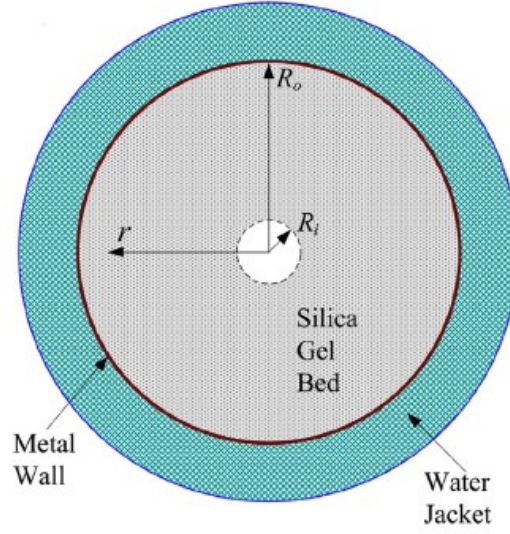


Figure 2.3: The cross-section of adsorbent bed considered here. Picture taken from *Wu, Biggs, Hu, 2014 (Ref. [1])*

2.2.2 Mathematical Modeling

Adsorption equilibrium and Mass transfer

As reported by J.W. Wu et al. (2014), in AD system is usual to describe the overall mass transfer in the silica gel bed by the equation

$$\epsilon_t \frac{\partial \rho_v}{\partial t} + (1 - \epsilon_t) \rho_{sg} \frac{\partial X}{\partial t} = -\frac{1}{r} \frac{\partial (r \rho_v u)}{\partial r} \quad (2.1)$$

In (2.1) ρ_v and ρ_{sg} are the density of the vapour and the silica gel particle, respectively; $\epsilon_t = \epsilon_{bed} + (1 - \epsilon_{bed}) \cdot \epsilon_{pa}$ is the total porosity of the adsorbent bed, including the fraction of the bed volume that is occupied by the voids (ϵ_{bed}) and the fraction occupied by the silica gel particles (ϵ_{pa}); u is the vapour velocity in the bed and it can be evaluated by Darcy's Law, considering the vapour viscosity, the pressure, the bed permeability and the particles diameter.

$\frac{\partial X}{\partial t}$ is the rate of water uptake and, finally, r is the radial coordinate used to analyzed the transfer problem. In order to reduce the computational cost, intraparticle mass diffusion is not explicitly resolved; in particular, referring to the linear driving force equation (LDF) proposed by Sakoda and Suzuki (1984), surface diffusion dominates intraparticle mass transport, which means that the adsorption rate is controlled by the adsorbate gas diffusion in the adsorbent particle. Therefore, to model the mass

transfer within silica gel, the rate of water uptake is given by

$$\frac{\partial X}{\partial t} = \frac{15D_{so}}{\frac{1}{2}d_{pa}^2} \exp\left(\frac{-E_a}{RT}\right) (X^* - X) \quad (2.2)$$

where D_{so} is the pre-exponential constant, d_{pa} is the average adsorbent bed particles diameter, E_a is the activation energy of diffusion, R is the universal gas constant, T is the temperature, X is the mean adsorbed concentration within the particle and X^* is mass fraction of adsorbed water at equilibrium and it is a function of a given temperature and bulk phase pressure ($X^* = f(T, P)$). To find out the X^* value of the rate of water uptake at equilibrium, various studies employ a methodical approach based on the experimental consideration of linear adsorption isotherms.

In this thesis work it has been used a numerical approach as follows.

As a first approximation to better understand the problem physics and order of size, the adsorption equilibrium is described by

$$X^* = k \left(\frac{P}{P_s}\right)^{1/n} \quad (2.3)$$

as reported in Sakoda and Suzuki (1984) research. In (2.3), X^* is the amount of water adsorbed in equilibrium with pressure P , P_s is the saturation vapour pressure and k and n are two constants that depend on the adsorbate-adsorbent pair.

In particular, the relation given by Eq. (2.3) can be expressed as a function of the temperature of adsorbate in the liquid phase, T_w , and the temperature in the bed, T_s :

$$X^* = k \left(\frac{P_s(T_w)}{P_s(T_s)}\right)^{1/n} \quad (2.4)$$

where $P_s(T_w)$ and $P_s(T_s)$ are the saturation vapour pressures at the temperatures T_w and T_s , respectively; they are calculated by using the Antoine's equation.

The limitation in Eq. (2.4) is that there is not explicitly highlighted the total pressure of the system. Thus, X^* is calculated by the Dubinin-Astakhov (D-A) equations, which are:

$$X^* = X_0 \exp\left[-k \left(\frac{T}{T_s} - 1\right)^n\right] \quad (2.5)$$

$$X^* = X_0 \exp\left[-D \left(T \ln \frac{P_s}{P}\right)^n\right] \quad (2.6)$$

where X_0 , k and D are coefficients, different for the various working pairs but also different according to the brand and type of the adsorbent chosen; T is the

adsorption temperature; T_s is the saturated temperature of refrigerant; P_s is the saturated pressure of refrigerant; P is the pressure of the system.

To conclude this discussion, considering the cycle diagram shown in Figure 1.6 and the study of J.W. Wu et al. (2010), the mass of fresh water generated in a single cycle from one bed can be evaluated as

$$m_{water} = \Delta m_{2-3} = m_2 - m_3 = X_2 m_{sg} - X_3 m_{sg} \quad (2.7)$$

where m_{sg} is the mass of adsorbent material in one single bed; Δm_{2-3} is the water productivity and so the water obtained at the end of the process; X_2 and X_3 are the adsorbed phase concentration at equilibrium for state 2 and 3, respectively, which can be calculated by using Eq. (2.5) or (2.6).

Heat transfer

To continue the analysis of the system, it is relevant to focus on the thermal energy that is required for the regeneration of the adsorbent bed and, at the same time, the one released during the adsorption process. Consequently, considering always the assumptions listed below, here is reported the expression for heat transfer in the radial direction through the bed:

$$(\rho C)_{eq} \frac{\partial T}{\partial t} = k_{eq} \frac{\partial^2 T}{\partial r^2} + \frac{k_{eq}}{r} \cdot \frac{\partial T}{\partial r} + \dot{q} \quad (2.8)$$

where k_{eq} is the effective thermal conductivity of the bed and \dot{q} is the rate of heat generation due to sorption. Moreover, the term $(\rho C)_{eq}$ is the effective total heat capacity of the bed, calculated as the mass-weighted average of the heat capacities of the single components of the bed, so silica gel, adsorbed water and vapour:

$$(\rho C)_{eq} = (1 - \epsilon_t) \rho_{sg} C_{sg} + (1 - \epsilon_t) X \rho_{sg} C_w + \epsilon_t \rho_v C_v \quad (2.9)$$

Additionally, considering again the cycle diagram shown in Fig. 1.5 and the study of J.W. Wu et al. (2010), the total heating requirement of a single cycle is expressed by:

$$Q_{heating(bed)} = Q_{1-2} + Q_{2-3} \quad (2.10)$$

In particular,

$$Q_{1-2} = (X_1 m_{sg} C_w + m_{sg} C_{sg})(T_2 - T_1) \quad (2.11)$$

and

$$Q_{2-3} = \left[m_{sg} C_{sg} + \left(\frac{X_2 + X_3}{2} \right) m_{sg} C_{sg} \right] (T_3 - T_2) + (X_2 - X_3) m_{sg} Q_{des} \quad (2.12)$$

In Eq. (2.11) and (2.12) $T_1, T_2, T_3, X_1, X_2, X_3$ are the temperatures and the adsorbed phase concentration at equilibrium for state 1, 2 and 3, respectively; C_w and C_{sg} are the specific heat of water and silica gel, respectively; Q_{des} is the amount of heat required per kg of water to activate the desorption process.

Q_{2-3} describes the heat required for the isobaric heating/desorption process; it consists of two parts: firstly, the heat necessary to increase the temperature of the bed and the water adsorbed on it, secondly, the latent heat indispensable to drive the water off the silica gel.

In a similar manner, the cooling requirement of a single cycle for the bed is expressed by:

$$Q_{cooling}(bed) = Q_{3-4} + Q_{4-1} \quad (2.13)$$

In particular,

$$Q_{3-4} = (X_3 m_{sg} C_w + m_{sg} C_{sg})(T_3 - T_4) \quad (2.14)$$

and

$$Q_{4-1} = \left[m_{sg} C_{sg} + \left(\frac{X_4 + X_1}{2} \right) m_{sg} C_{sg} \right] (T_4 - T_1) + (X_1 - X_4) m_{sg} Q_{ads} \quad (2.15)$$

In Eq. (2.14) and (2.15) $T_1, T_3, T_4, X_1, X_3, X_4$ are the temperatures and the adsorbed phase concentration at equilibrium for state 1, 3 and 4, respectively; Q_{ads} is the amount of heat released per kg of water. In this study, Q_{ads} , Q_{des} and Q_{st} (which is the isosteric heat of adsorption) are assumed to be equal to each other.

As Q_{2-3} , also Q_{4-1} , that is the heat involved in the isobaric cooling/adsorption process, consists of two parts; firstly, the heat necessary to increase the temperature of the bed and the water adsorbed on it, secondly, the latent heat to drive the water evaporating from liquid to vapour form.

Finally, to quantify the benefit obtained in the chiller mode, the cooling effect in the evaporator can be expressed as

$$Q_{evap} = m_{sg} (X_1 - X_4) h_{fg}^4 \quad (2.16)$$

where h_{fg}^4 is the specific phase change enthalpy at the evaporator pressure.

Coefficient of performance

One of the indicators commonly used to evaluate the efficiency of such a system is the COP or Coefficient of Performance for the process described; in this work, COP

is calculated including the cooling effect at the evaporator; recalling that the cold production that takes place in the evaporator is given by Eq. (2.16) and referring to Eq. (2.10), Eq. (2.11) and Eq. (2.12),

$$COP = \frac{Q_{evap}}{Q_{heating(bed)}} \quad (2.17)$$

and it can be seen as the useful energy effect divided the energy required to obtain it.

Initial and boundary conditions

Considering the AD cycle diagram in Fig 1.5, that starts at point 1, the initial conditions are:

$$T(t = 0, r) = T_{cw} \quad (2.18)$$

$$P(t = 0, r) = P_0 \quad (2.19)$$

$$X(t = 0, r) = X^* \quad (2.20)$$

where T_{cw} is the cooling water temperature and P_0 is the initial bed pressure.

Instead, the first boundary condition for pressure is

$$\left. \frac{\partial P}{\partial r} \right|_{r=R_0} = 0 \quad (2.21)$$

Then, depending on whether the core is connected to the condenser (process 2 → 3) or the evaporator (process 4 → 1), one has

$$P(t, r = R_i) = P_{cond} \quad (2.22)$$

$$P(t, r = R_i) = P_{evap} \quad (2.23)$$

respectively.

Moreover, the two boundary conditions for temperature are

$$\left. \frac{\partial T_{sg}}{\partial r} \right|_{r=R_i} = 0 \quad (2.24)$$

$$-k_{sg} \left. \frac{\partial T_{sg}}{\partial r} \right|_{r=R_0} = h_{m,sg}(T_m - T_{sg}) \quad (2.25)$$

Then, during the process 1 → 2 → 3 (heating phase)

$$T_f = T_{hw} \quad (2.26)$$

and during the process 3 → 4 → 1 (cooling phase)

$$T_f = T_{cw} \quad (2.27)$$

In the Equations above, k_{sg} is the silica gel thermal conductivity; $h_{m,sg}$ is the metal to silica gel heat transfer coefficient; T_{cw} is the cooling water temperature while T_{hw} is the hot water one; T_f is the temperature of the fluid circulating in the water jacket; T_m is the metal wall temperature.

In addition, another boundary condition is imposed on the heat flux generated by the evacuated solar panels, at the outer radius R_0 ; it is considered as an heat external source of a given variable value HF, as follows

$$\dot{q}|_{r=R_0} = HF \quad (2.28)$$

2.3 Tools and solution methodology

The model described above is numerically solved using Matlab & Simulink. As a general rule, Matlab solver uses finite differences methods for the differential equations and first or second order forward difference schemes to discretise the time derivatives and boundary conditions; moreover, the spatial derivatives are discretised using second order central difference schemes.

In this thesis work, the Matlab Partial Differential Equation Toolbox is used, particularly to study the heat transfer problem: a thermal analysis model is created, including all the elements listed in the previous paragraphs (geometry, thermal properties, initial and boundary temperature conditions, heat flux through the boundaries and mesh). The first step is to import the geometry and plot it; then, starting from the default toolbox setup, the parameters must be modified and adapted to the problem in question:

- Thermal properties: Indicate the thermal conductivity, the mass density and the specific heat of the material;
- Boundary conditions: Specify the temperature and the heat flux on each edge or face of the geometry object;
- Initial conditions: Set the initial value of the bed temperature;
- Mesh: Generate a mesh with triangular elements, then plot it using *pdemesh* and *pdeplot* functions;
- Solution times: Define a cycle time and specify time steps to calculate solution;

- Solution: Use the *solve* function to obtain the thermal results of the discussed problem; note that the solution can be a steady-state or a transient one, according to the initial hypothesis;
- Temperature profile: Plot the solution at the final time step and the temperature distribution, using the *contour* and *colormap* plot.

Figure 2.4 and Figure 2.5 depict the geometry of the thermal object created; cell and edge labels are shown to better understand where the boundary conditions are applied.

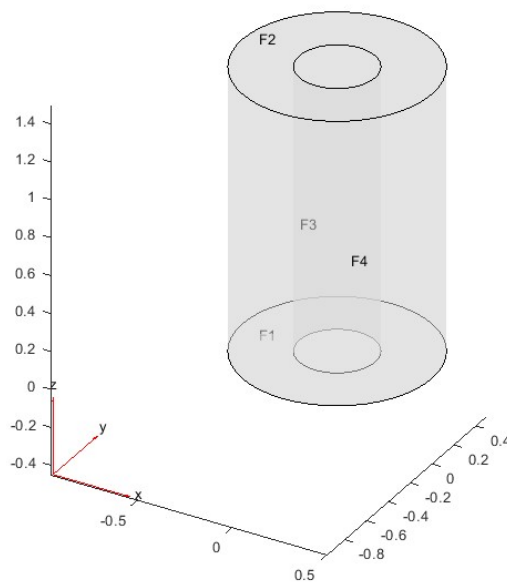


Figure 2.4: Hollow cylindrical thermal object, representing the core of the system, cell labels on

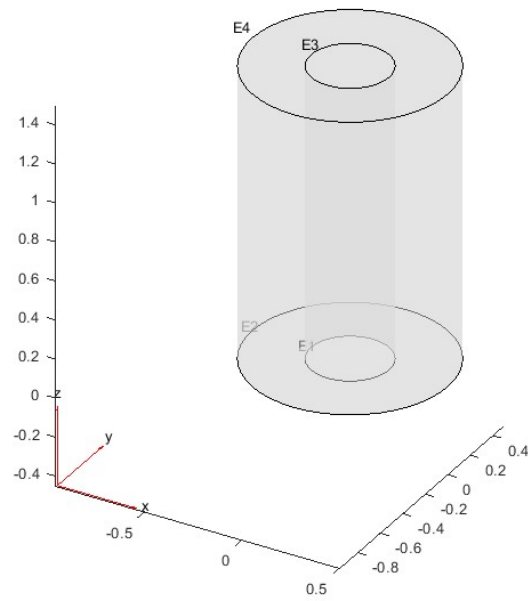


Figure 2.5: Hollow cylindrical thermal object, representing the core of the system, edge labels on

From this geometry, mesh is generated and plotted, as illustrated in Figure 2.6; then, considering that heat (and mass) transfer is a radial phenomenon, the 3-D problem is switched to a 2-D one and related mesh is shown in Figure 2.7.

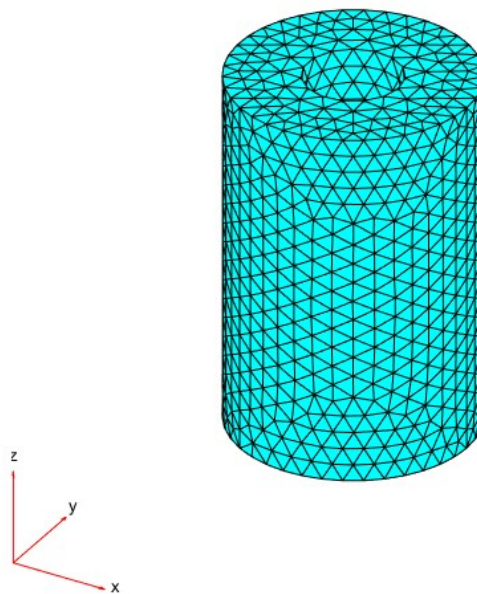


Figure 2.6: Mesh with triangular elements, 3-D problem

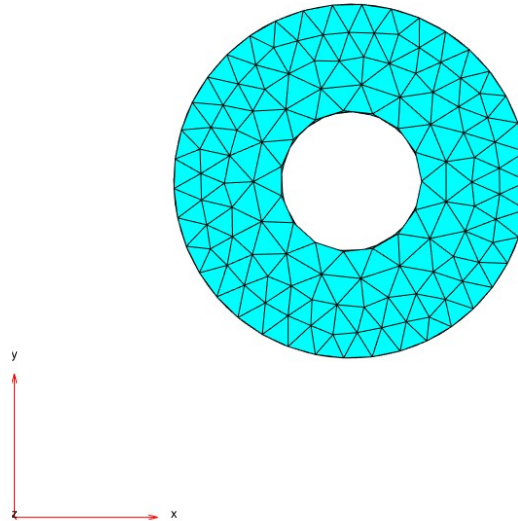


Figure 2.7: Mesh with triangular elements, 2-D problem

In this way, considering a 2-D problem, rather than a 3-D one, there is a reduction in computational costs and in terms of time required to reach the solution for a single numerical simulation.

As regards the adsorption equilibrium and the mass transfer, they are solved using simultaneously Matlab and Simulink, with the *ode45* solver function. Figure 2.8 displays a screenshot of the Simulink layout, with an evidence on the main subsystems in which the mathematical model is divided.

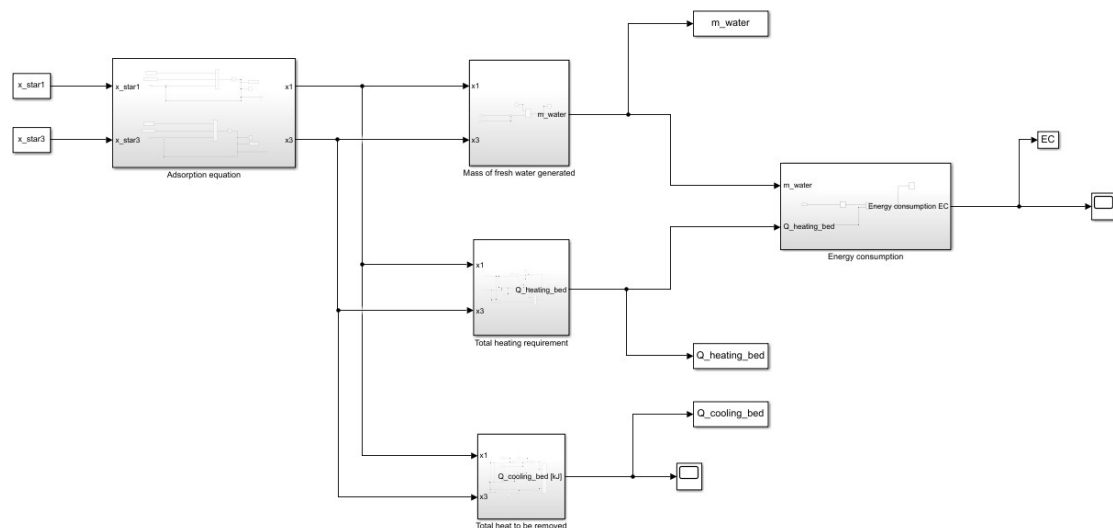


Figure 2.8: Simulink layout for solving the adsorption equations

To conclude this chapter and to sum up all the numerical values, Table 2.1 lists the

major constant parameters assumed for the problem. Notice that, in respect with the assumptions of the considered equations, the total pressure of the system may be varied between 1000 and 1500 Pa; it is proved that this thesis project numerical model works correctly.

Property	Symbol	Value
Number of time steps	nt	200
Number of radial subdivisions	n	200
Silica gel bulk density	ρ_{sg}	2027 kg/m ³
Zeolite bulk density	ρ_z	620 kg/m ³
Water vapour density	ρ_v	0,15 kg/m ³
Silica gel specific heat	C_{sg}	920 J/(kgK)
Zeolite specific heat	C_z	836 J/(kgK)
Water vapour specific heat	C_v	1920 J/(kgK)
Water specific heat	C_w	4185,5 J/(kgK)
Effective bed thermal conductivity	k_{eq}	0,175 W/(mK)
Heat transfer coefficient	$h_{m,sg}$	36 W/(m ² K)
Silica gel + water system heat of adsorption	$Q_{st,sg}$	2800 kJ/kg
Zeolite + water system heat of adsorption	$Q_{st,z}$	3110 kJ/kg
Pre-exponent constant	D_{so}	$2,5 \times 10^{-4}$ m ² /s
Silica gel activation energy of diffusion	$E_{a,sg}$	$4,2 \times 10^4$ J/mol
Zeolite activation energy of diffusion	$E_{a,z}$	$4,55 \times 10^4$ J/mol
Core inner radius	R_i	0,2 m
Core outer radius	R_o	0,5 m
Average silica gel particle diameter	$d_{pa,sg}$	$3,4 \times 10^{-4}$ m
Average zeolite particle diameter	$d_{pa,z}$	2×10^{-4} m
Silica gel bed porosity	$\epsilon_{bed,sg}$	0,37
Zeolite bed porosity	$\epsilon_{bed,z}$	0,25
Bed initial temperature	T_{in}	15 °C
Cycle time	T_{cycle}	3000 s
D-A equations parameters		
For silica gel	n	1,7
	D	6×10^{-6}
	x_0	0,35
For zeolite	n	1,73
	k	5,36
	x_0	0,261

Table 2.1: Model parameters

Chapter 3

Results

Basing on the methods enunciated in the previous chapter, the results of the analysis of the solar powered adsorption desalination and cooling system presented here are reported below.

First of all, various simulations have been done and compared together, in order to evaluate one of that geometric configurations, among the many, that allows to obtain great performance, especially in terms of fresh water production and maximum temperature at the external surface. Then,

$$R_i = 0,2 \text{ m}$$

$$R_o = 0,5 \text{ m}$$

Secondly, silica gel and zeolite have been compared too, in order to identify the adsorbent material that fits better into the current case of study. After a lot of simulations, silica gel has proven to be the best between these two. Therefore, all the observations and results stated below are referred to silica gel as bed adsorbent material.

3.1 Heat flux influence on the system performance

For a given evaporation temperature and total pressure of the system, the mass of fresh water generated in a single cycle from one bed, the total heating requirement of a single cycle and, analogously, the cooling requirement of a single cycle are investigated. In particular, it has been analysed how these quantities vary when the heat flux, coming from the solar panels, changes; its value is set between 500 and

1000 W/m² and it is supposed, for simplicity, a solar panels area of 1 m².

Now, assuming

$$T_{evap} = 20^{\circ}\text{C}$$

and

$$P = 1000 \text{ Pa}$$

the following figures depict the results.

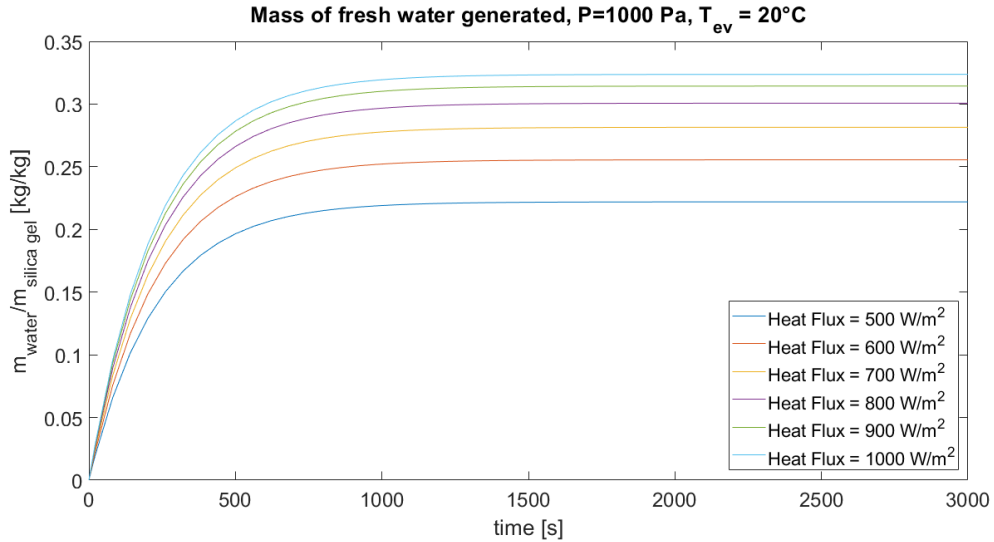


Figure 3.1: Mass of water generated in a single cycle from one bed, as a function of the Heat Flux

As shown in Figure 3.1 and Figure 3.2, the amount of water generated at the final time (3000 s), called from now as m_{water}^* or amount of water after the transient gap, increases with the increment of solar flux; in other words, the bigger is the heat flux, the higher is the water production rate. The same comment is valid for the quantity of heat supplied for the desorption process and released during the adsorption one; it can be noticed that, obviously, heat supplied is greater than heat released. Moreover, theoretically, even if the evolution shape of the two forms of heat is qualitatively the same, the slope of the two curves is slightly different: in fact, during the desorption process, starting from cooling initial conditions, firstly the dynamics of the system is slower and then more rapid; on the contrary, when heat is subtracted, starting from hot initial conditions and high temperature gradients, firstly the dynamics is faster and then, due to heat transfer, gradually the system cools down. This phenomenon is not clearly evident because of the the working temperature range considered here. Considering the coefficient of performance of the process, including the cooling effect from the evaporator, the trend is the opposite compared to what has been said just

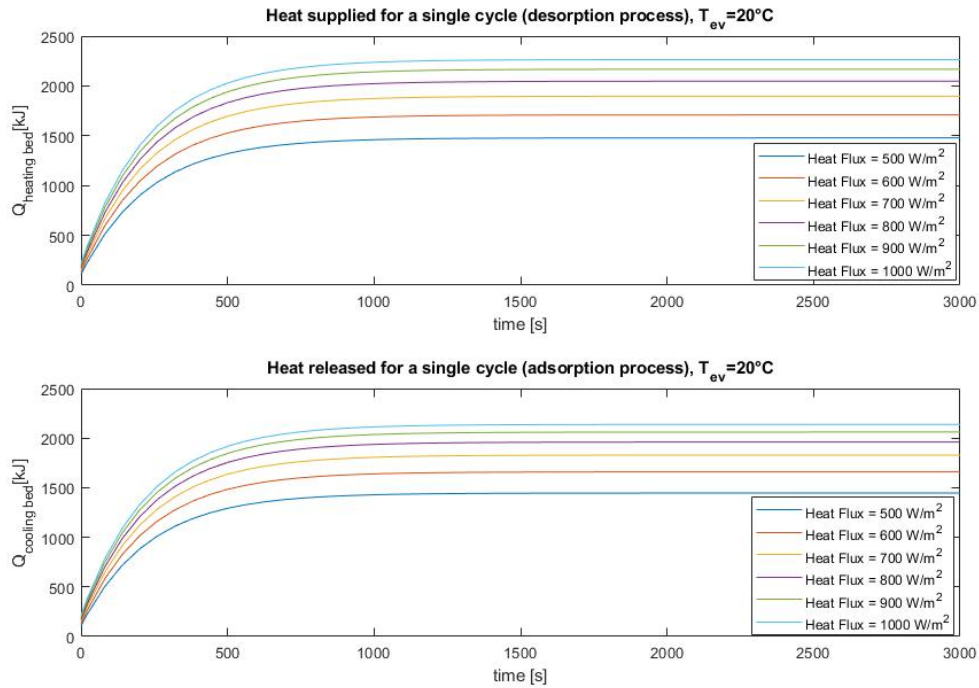


Figure 3.2: Total heating and cooling requirement of a single cycle, as a function of the Heat Flux

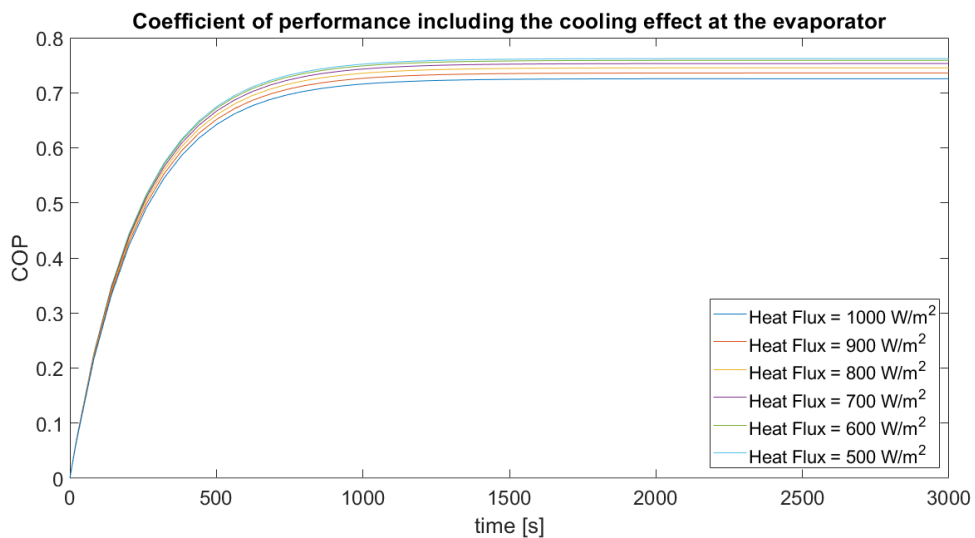


Figure 3.3: Coefficient of performance of the process, as a function of the Heat Flux

now, as shown in Figure 3.3. So, the bigger is the heat flux, the smaller is the system COP and this is reasonable because, when the solar flux increases, under the same useful energy effect, energy required to obtain it increases too.

As a consequence, one has to choose a proper trade-off between the two useful effects, in terms of water production and efficiency of the process (Figure 3.4).

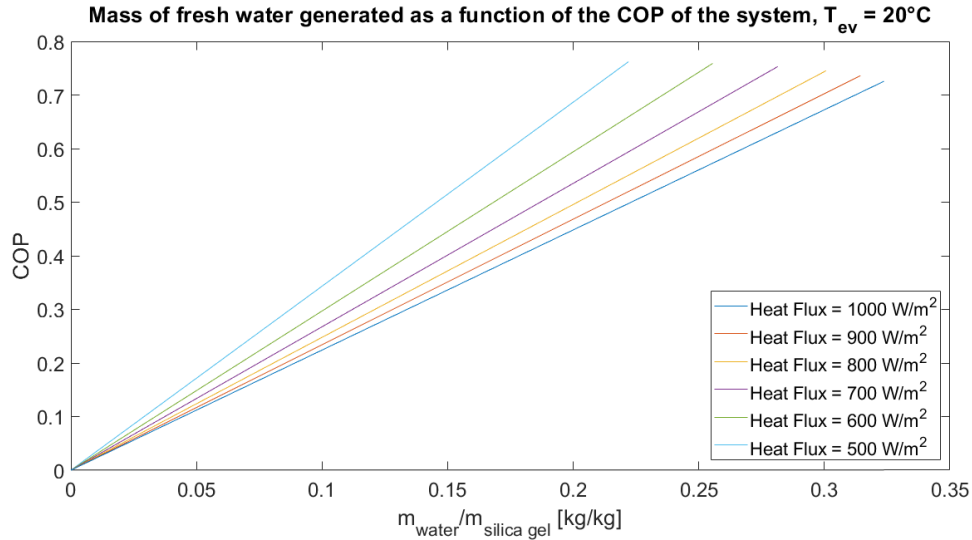


Figure 3.4: Coefficient of performance of the process as a function of the water production

The same graphics have been derived varying the bed total pressure (from 1000 Pa to 1400 Pa) and they are reported in the Appendix, for grater clarity. However, numerical results are collected in the tables below (Table 3.1 and Table 3.2).

COP	Heat Flux [W/m^2]					
Pressure [Pa]	500	600	700	800	900	1000
1000	0,762098	0,758913	0,75312	0,745314	0,735979	0,725533
1100	0,759464	0,757032	0,751829	0,744498	0,735547	0,725409
1200	0,756763	0,75508	0,750454	0,743583	0,735003	0,725161
1300	0,753994	0,753062	0,749008	0,742587	0,734366	0,72481
1400	0,751154	0,750981	0,747496	0,741518	0,733648	0,72437

Table 3.1: Coefficient of performance, including the cooling effect at the evaporator, at final time (3000 s) for a fixed evaporation temperature (20°C), varying heat flux and pressure of the system

$m_{\text{water}}/m_{\text{sg}}$	Heat Flux [W/m^2]					
Pressure [Pa]	500	600	700	800	900	1000
1000	0,221995	0,255527	0,281489	0,300697	0,314346	0,323694
1100	0,219062	0,253597	0,28059	0,300744	0,315193	0,325177
1200	0,21587	0,251303	0,27924	0,300274	0,315478	0,326069
1300	0,212473	0,248713	0,27752	0,299377	0,315294	0,326465
1400	0,208905	0,245876	0,275486	0,298114	0,314708	0,326434

Table 3.2: Mass of fresh water generated, at final time (3000 s) for a fixed evaporation temperature (20°C), varying heat flux and pressure of the system

Finally, to summarize the results illustrated before, combining different total

pressures and heat fluxes through the external cylindrical surface, it can be remarkable to plot COP and m_{water} value at the equilibrium or, in other words, at the final simulation time (Figure 3.5 and Figure 3.6).

The bigger is the total pressure of the system, the smaller is the COP of the process and the water production; this trend is more noticeable with the lower heat fluxes; as a consequence, so much greater is the depression, so much better performs the plants.

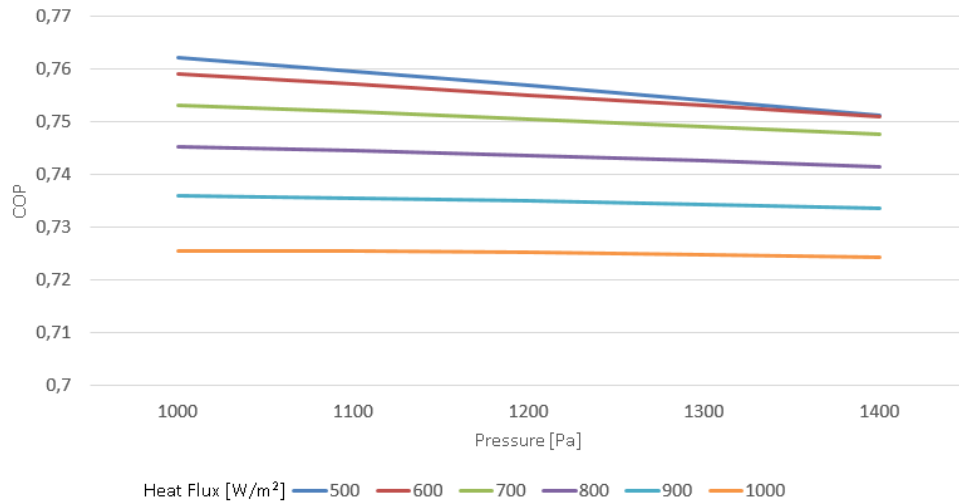


Figure 3.5: Coefficient of performance at final time (3000 s), for different pressures and heat fluxes, $T_{\text{evap}} = 20^\circ\text{C}$

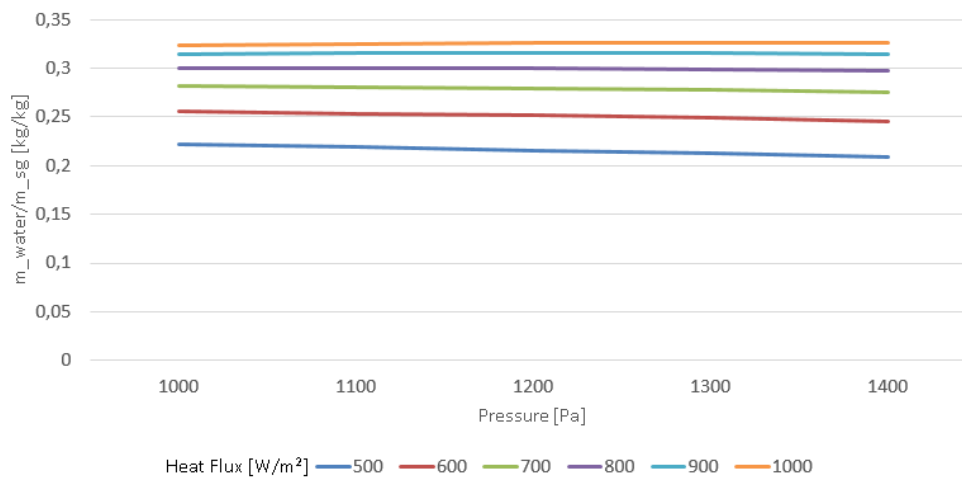


Figure 3.6: Mass of fresh water generated at final time (3000 s), for different pressures and heat fluxes, $T_{\text{evap}} = 20^\circ\text{C}$

3.2 Evaporation temperature influence on the system performance

For a given heat flux and total pressure of the system, the mass of fresh water generated in a single cycle from one bed, the total heating requirement of a single cycle and, analogously, the cooling requirement of a single cycle are investigated. In particular, it has been analysed how these quantities vary when the temperature of water, charged into the evaporator device, changes; its value is between 5 and 40 °C.

Now, assuming

$$\text{Heat Flux} = 500 \text{ W/m}^2$$

and

$$P = 1000 \text{ Pa}$$

the following figures highlight the results. As shown in Figure 3.7 and Figure

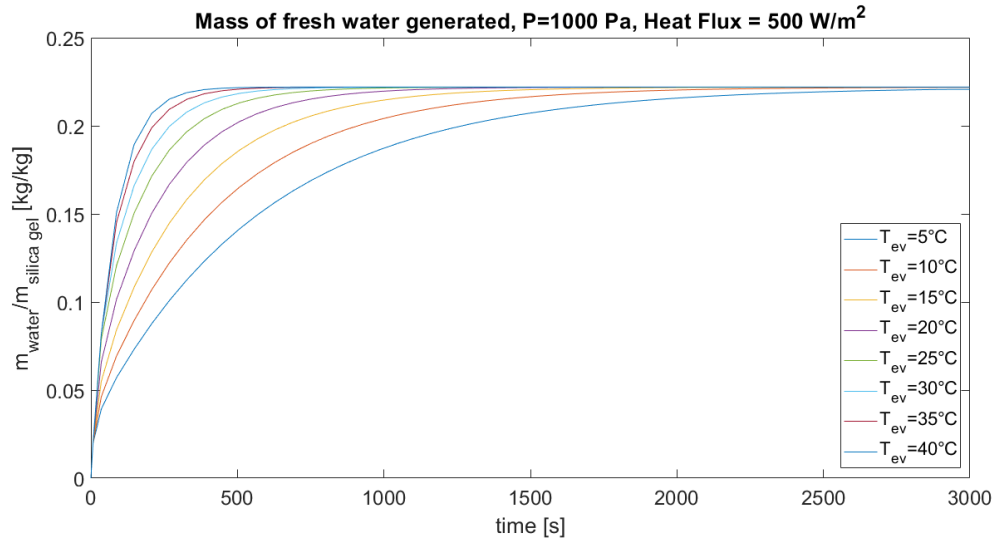


Figure 3.7: Mass of water generated in a single cycle from one bed, as a function of the evaporator temperature

3.8, the amount of water generated at the final time (3000 s), differently from the previous discussion, do not increase with the increment of evaporation temperature; in other words, even if the temperature imposed at the evaporator is raised up, the water production rate do not change significantly. The same comment is valid for the quantity of heat supplied for the desorption process and released during the adsorption one. The tangible difference between the various curves plotted is that

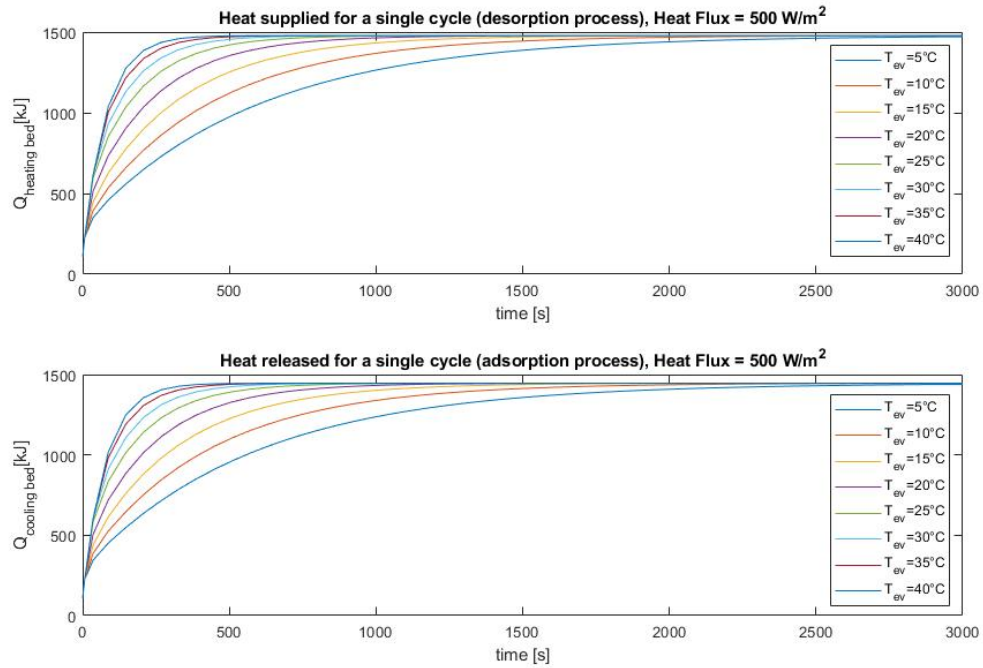


Figure 3.8: Total heating and cooling requirement of a single cycle, as a function of the evaporator temperature

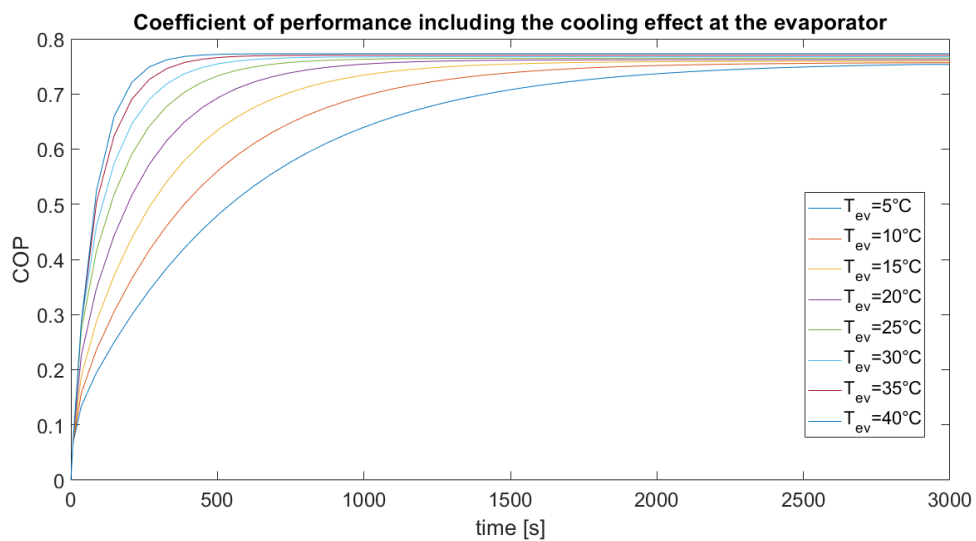


Figure 3.9: Coefficient of performance of the process, as a function of the evaporator temperature

the higher is the evaporator temperature, the lower is the time required to reach the equilibrium values of the three physical quantities under investigation. Considering the coefficient of performance of the process, including the cooling effect from the evaporator, the trend is identical to what has been said just now, as shown in Figure 3.9. So, the bigger is the evaporation temperature, the smaller is the time required

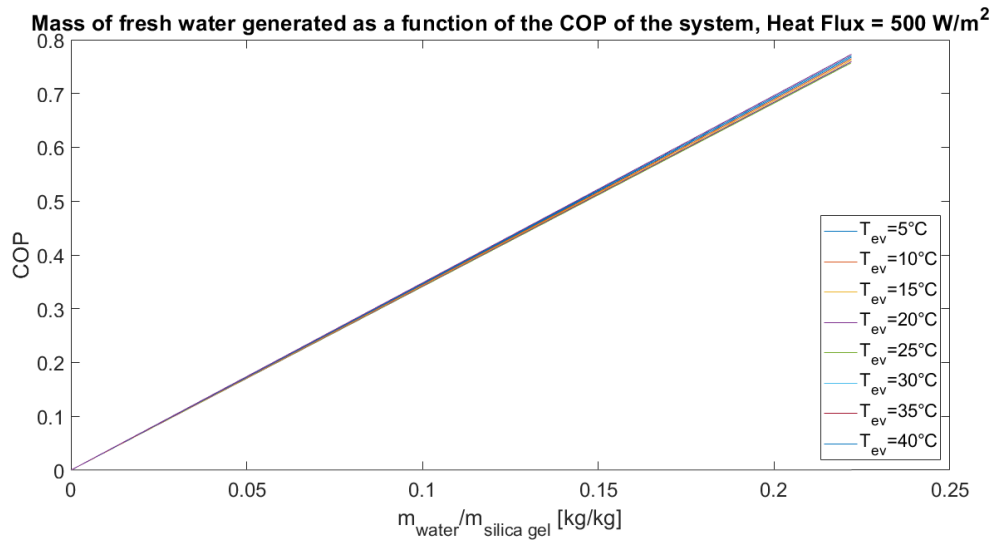


Figure 3.10: Coefficient of performance of the process as a function of the water production

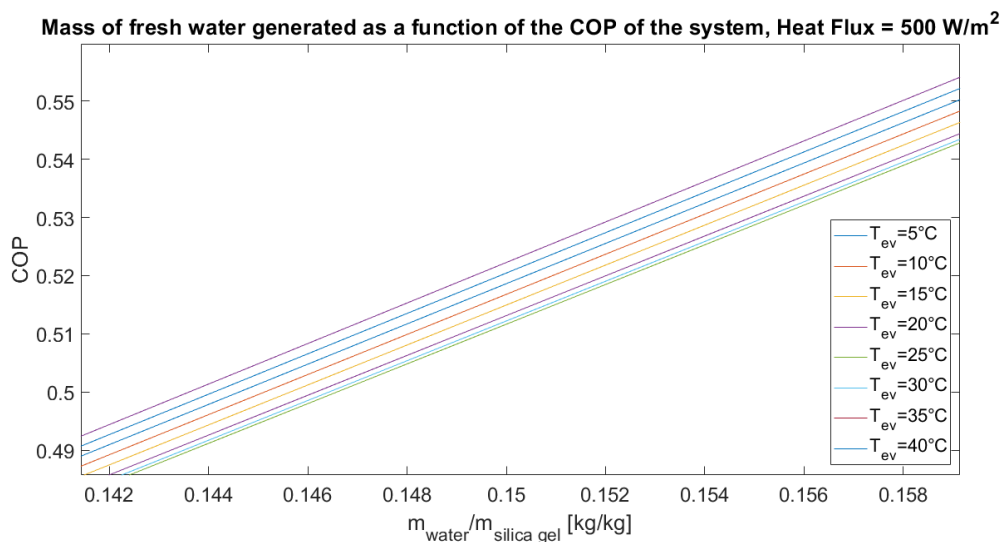


Figure 3.11: Coefficient of performance of the process as a function of the water production, zoom of Fig. 3.10

to obtain the equilibrium COP value.

Hence, to vary the heat flux on the external surface of the core has a great influence on the effective value of the quantities analysed, whereas the variation of the evaporation temperature causes effects on the dynamics of the process. From Figure 3.10 and Figure 3.11 it is evident what has been previously said.

As well as before, the same graphics have been derived varying the bed total pressure (from 1000 Pa to 1500 Pa) and they are reported in the Appendix, for grater clarity; however, numerical results are collected in the tables below (Table 3.3 and

Table 3.4).

COP	T_{evap} [°C]							
Pressure [Pa]	5	10	15	20	25	30	35	40
1000	0,753543	0,756573	0,75936	0,762098	0,764823	0,767538	0,770241	0,772931
1100	0,750936	0,753958	0,756735	0,759464	0,76218	0,764885	0,767579	0,77026
1200	0,748261	0,751576	0,754044	0,756763	0,759469	0,762165	0,764849	0,767521
1300	0,745519	0,748607	0,751285	0,753994	0,756691	0,759376	0,762051	0,764713
1400	0,742707	0,745707	0,748455	0,751154	0,75384	0,756516	0,75918	0,761832
1500	0,739814	0,742806	0,745545	0,748233	0,750909	0,753574	0,756229	0,75887

Table 3.3: Coefficient of performance, including the cooling effect at the evaporator, at final time (3000 s) for a fixed heat flux (500 W/m^2), varying evaporation temperature and pressure of the system

$m_{\text{water}}/m_{\text{sg}}$	T_{evap} [°C]							
Pressure [Pa]	5	10	15	20	25	30	35	40
1000	0,220677	0,221805	0,221981	0,221995	0,221995	0,221995	0,221996	0,221996
1100	0,217762	0,218875	0,219048	0,219062	0,219062	0,219063	0,219063	0,219063
1200	0,214589	0,215686	0,215856	0,21587	0,215871	0,215871	0,215871	0,215871
1300	0,211212	0,212291	0,212459	0,212473	0,212473	0,212473	0,212473	0,212473
1400	0,207665	0,208727	0,208892	0,208905	0,208906	0,208906	0,208906	0,208906
1500	0,203969	0,205012	0,205174	0,205187	0,205188	0,205188	0,205188	0,205188

Table 3.4: Mass of fresh water generated, at final time (3000 s), for a fixed heat flux (500 W/m^2), varying evaporation temperature and pressure of the system

Finally, to summarize the results illustrated before, combining different total pressures and evaporation temperatures, it can be interesting to plot COP and m_{water} value at the equilibrium or, in other words, at the final simulation time (Figure 3.12 and Figure 3.13). The bigger is the total pressure of the system, the smaller is the COP of the process and the water production, for a given evaporation temperature; moreover, for a given pressure, COP softly increases with the increase of evaporation temperature, but this trend is not too noticeable for the amount of fresh water generated, that seems to be quite independent from evaporation temperature (except in the case of T_{evap} equals to 5°C); as a consequence, as already explained before, so much greater is the depression, so much better performs the plants.

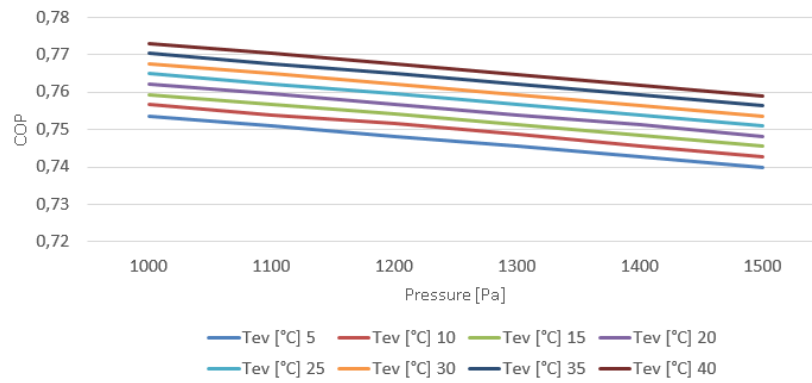


Figure 3.12: Coefficient of performance at final time (3000 s), for different pressures and evaporation temperature, Heat Flux = 500 W/m²

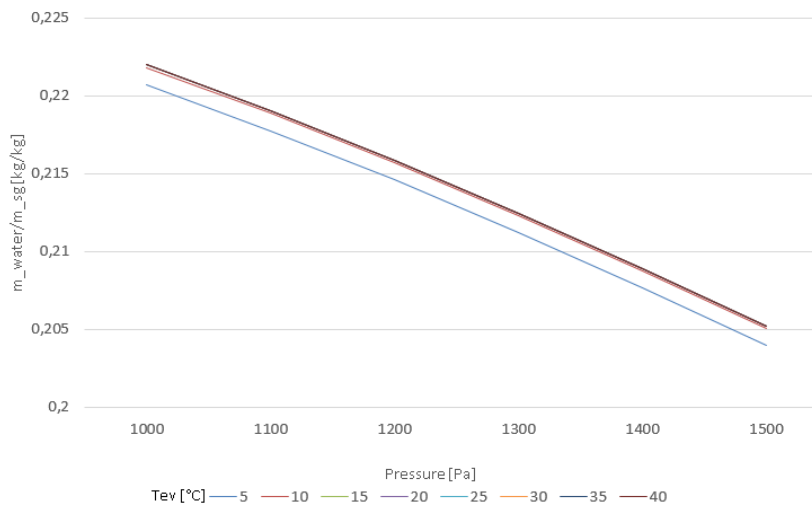


Figure 3.13: Mass of fresh water generated at final time (3000 s), for different pressures and evaporation temperature, Heat Flux = 500 W/m²

3.3 Temperature distribution and Temperature profile

As a result of the heat transfer problem, another important physical quantity is the maximum temperature reached by the system.

Referring to the case studied in section 3.1,

$$T_{evap} = 20^{\circ}\text{C}$$

$$P = 1000 \text{ Pa}$$

and

$$\text{Heat Flux} = [500 \ 600 \ 700 \ 800 \ 900 \ 1000] \text{ W/m}^2$$

in Figure 3.14 are portrayed the six temperature distributions for different heat flux conditions.

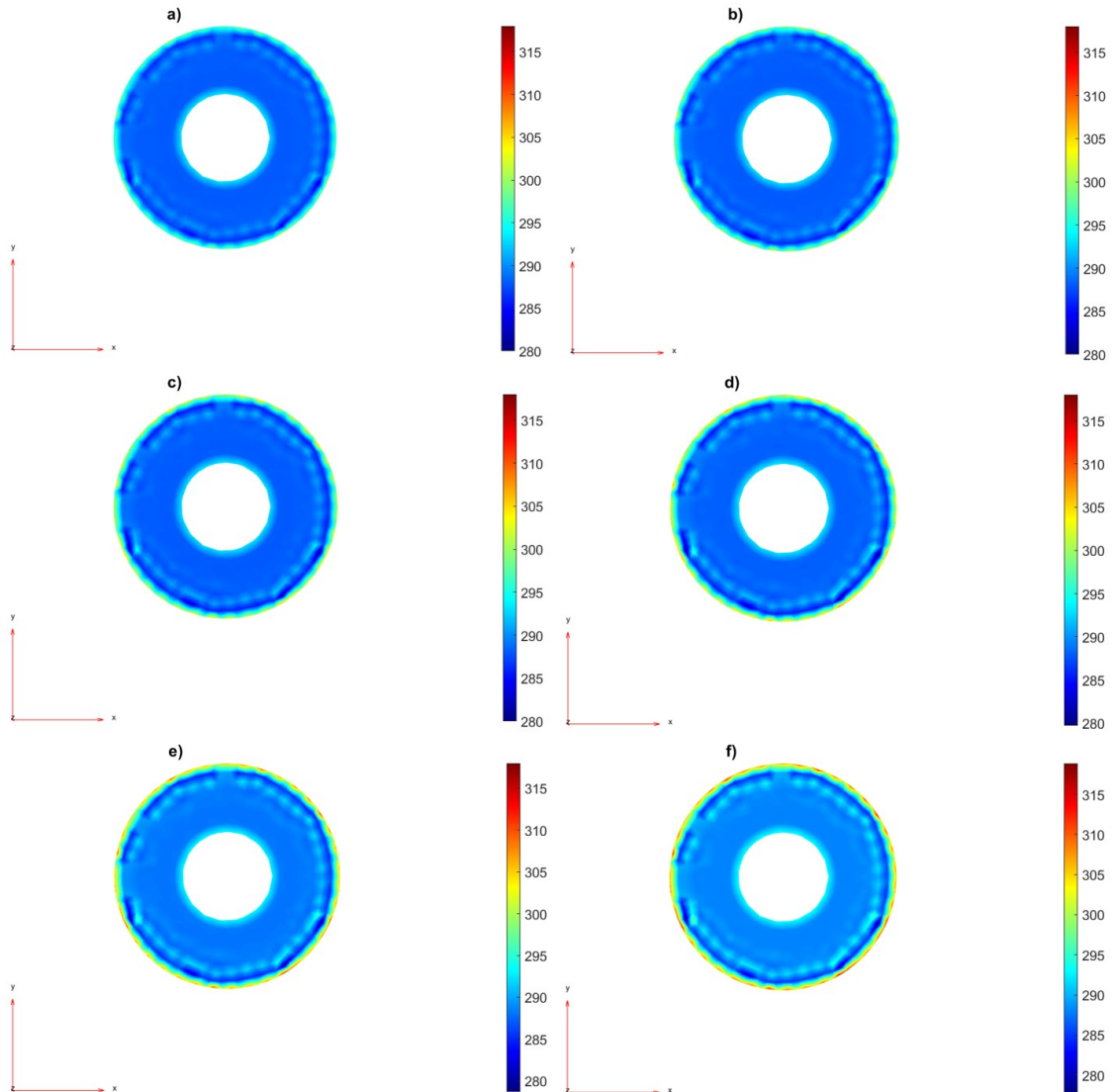


Figure 3.14: Temperature distribution for different heat fluxes: (a) 500 W/m^2 , (b) 600 W/m^2 , (c) 700 W/m^2 , (d) 800 W/m^2 , (e) 900 W/m^2 , (f) 1000 W/m^2

Analogously, referring to the case studied in section 3.2,

$$\text{Heat Flux} = 500 \text{ W/m}^2$$

$$P = 1000 \text{ Pa}$$

and

$$T_{evap} = [5 \ 10 \ 15 \ 20 \ 25 \ 30 \ 35 \ 40] \text{ } ^\circ\text{C}$$

then, Figure 3.15 depicts the eight temperature distributions for different evaporation temperature conditions.

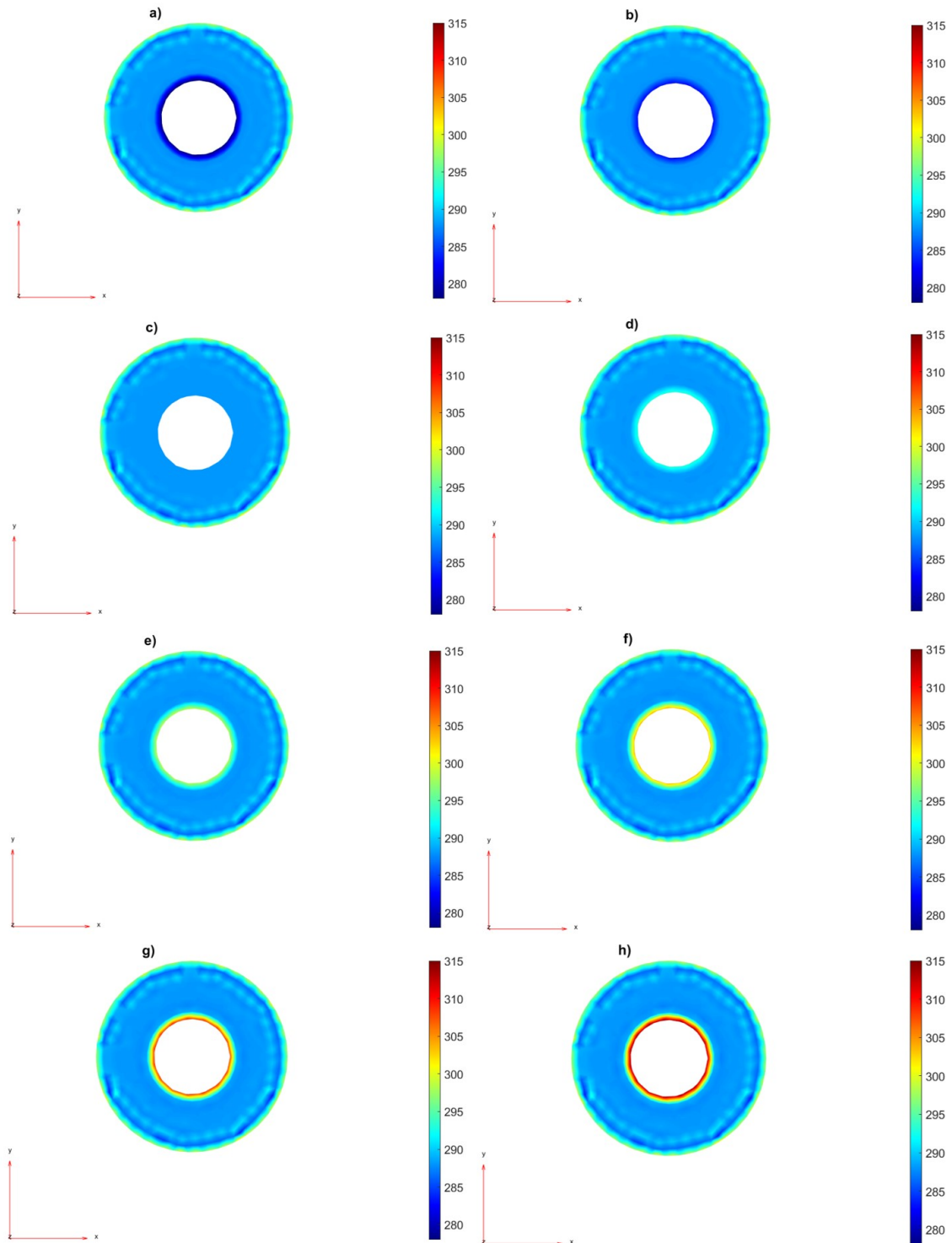


Figure 3.15: Temperature distribution for different evaporation temperatures: (a) 5 °C, (b) 10 °C, (c) 15 °C, (d) 20 °C, (e) 25 °C, (f) 30 °C, (g) 35 °C, (h) 40 °C

Moreover, for all the simulations done, it has been extrapolated the temperature profile at different radius value; this is a meaningful way to visualize how the temperature evolves, from the inner to the outer cylinder radius, and what is the maximum temperature value, reached by the core of the system. For all the combination of parameters examined, the curves result to have the same evolution; they differentiate each other only for the numerical values. For instance is now, finally, reported the typical temperature profile as a result of the heat transfer problem (Figure 3.16).

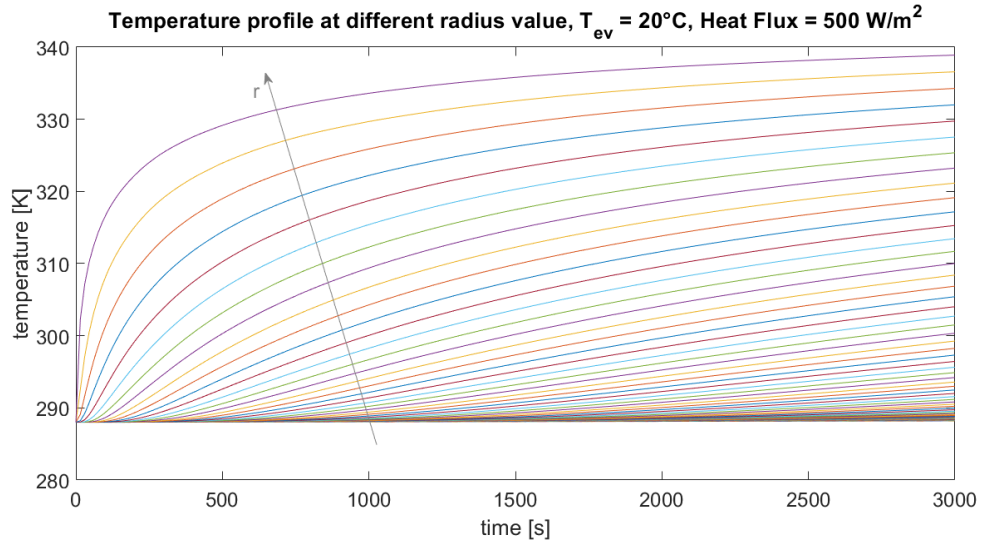


Figure 3.16: An example of one of the temperature profile at different radius value

In Table 3.5 the maximum temperatures reached on the external core surface, for a fixed heat flux of 500 W/m^2 , are listed and, then, reported graphically in Figure 3.17. Moreover, in this figure is also pictured a linear approximation curve to better underline the temperature evolution.

T_{\max} [K]	T_{evap} [°C]							
Pressure [Pa]	5	10	15	20	25	30	35	40
1000	338,893	338,893	338,893	338,893	338,893	338,893	338,893	338,893
1100	338,855	338,855	338,855	338,855	338,855	338,855	338,855	338,855
1200	338,815	338,815	338,815	338,815	338,815	338,815	338,815	338,815
1300	338,786	338,786	338,786	338,786	338,786	338,786	338,786	338,786
1400	338,759	338,759	338,759	338,759	338,759	338,759	338,759	338,759
1500	338,741	338,741	338,741	338,741	338,741	338,741	338,741	338,741

Table 3.5: Maximum temperature, reached on the external core surface, at final time (3000 s) for a fixed heat flux (500 W/m^2), varying evaporation temperature and pressure of the system

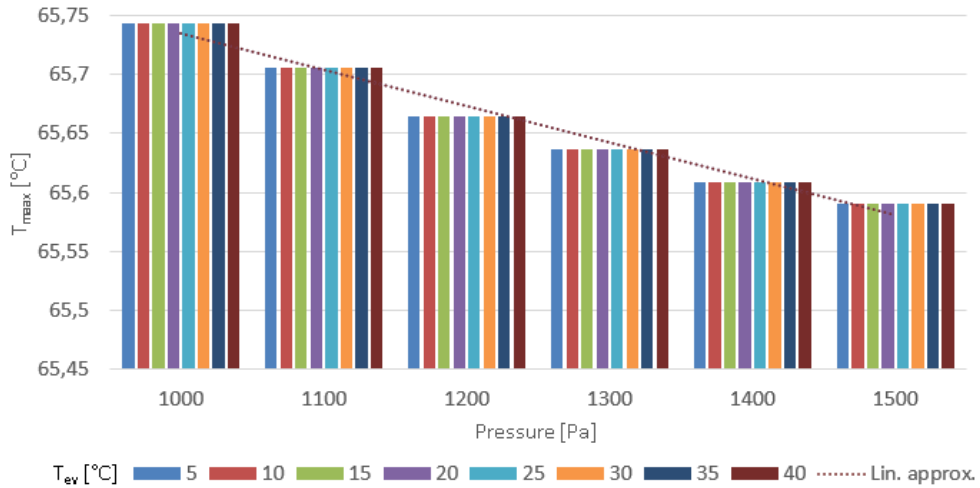


Figure 3.17: Evolution of the maximum temperature, reached on the external core surface (outer radius), at final time (3000 s) for a fixed heat flux (500 W/m^2), varying evaporation temperature and pressure of the system

It is quite clear that, for a fixed heat flux (here 500 W/m^2) and pressure, the maximum temperature, on the external core surface, is always the same, independently from the evaporation temperature; in addition, when pressure increases, temperature decreases but in a evident negligible manner.

By now, in Table 3.6 the maximum temperatures reached on the external core surface, for a fixed evaporation temperature ($20 \text{ }^\circ\text{C}$), are listed and, then, reported graphically in Fig. 3.18.

It may be highlighted that, for a fixed evaporation temperature and system pres-

T_{\max} [K]	Heat Flux W/m^2						
	Pressure [Pa]	500	600	700	800	900	1000
1000		338,893	349,246	359,616	369,985	380,346	390,691
1100		338,855	349,205	359,574	369,943	380,304	390,651
1200		338,821	349,168	359,537	369,906	380,268	390,616
1300		338,792	349,136	359,503	369,874	380,237	390,587
1400		338,765	349,107	359,474	369,845	380,21	390,56

Table 3.6: Maximum temperature, reached on the external core surface, at final time (3000 s) for a fixed evaporation temperature ($20 \text{ }^\circ\text{C}$), varying heat flux and pressure of the system

sure, the bigger the heat flux is, the higher the maximum temperature reached on the cylinder surface is (note that from 500 W/m^2 to 1000 W/m^2 there is an increment of approximately 50 K). At the same time, for a fixed evaporation temperature

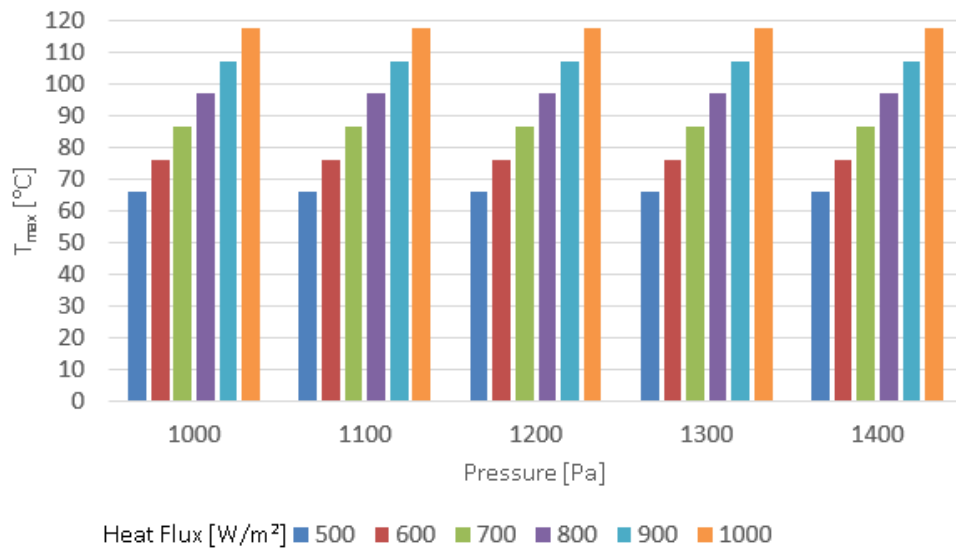


Figure 3.18: Evolution of the maximum temperature, reached on the external core surface (outer radius), at final time (3000 s) for a fixed evaporation temperature (20 °C), varying heat flux and pressure of the system

and heat flux, there is not a relevant maximum temperature variation varying the pressure of the system.

Chapter 4

Discussion and Conclusion

In this thesis project, the thermodynamic cycle of the adsorption desalination system is analyzed under defined equilibrium conditions, based on the study of various operating and performance parameters. The results of the problem, reported in Chapter 3, are in line with the ones elaborated in the previous studies by many investigators. In addition, to summarize the findings of this work:

1. For a fixed evaporation temperature and heat flux and for variable pressures of the system \rightarrow no relevant maximum temperature variation;
2. For a fixed heat flux and pressure of the system and for variable evaporation temperatures \rightarrow no maximum temperature variation;
3. For a fixed heat flux and pressure of the system and for variable evaporation temperatures \rightarrow mass of fresh water generated, heat supplied, heat released and COP (all values calculated at equilibrium) do not change meaningfully; the system dynamics is quicker when the evaporation temperature increases;
4. For a fixed evaporation temperature and pressure of the system and for variable heat fluxes \rightarrow maximum temperature increases with a solar flux increment;
5. For a fixed evaporation temperature and pressure of the system and for variable heat fluxes \rightarrow mass of fresh water generated, heat supplied and heat released (all values calculated at equilibrium) increase when heat flux increases too, while COP decreases;
6. For a variable pressure of the system \rightarrow performance parameters decrease.

It can therefore be concluded that the system presented here seems to have reasonable efficiency; in fact, independently from how the various parameters under

examination have been combined each other, the COP is between 0,72 and 0,78 and the amount of fresh water generated is between 20% and 35% of the total silica gel mass used in the model. Moreover, also the porosity of the bed has been analyzed but the COP does not change with the variation of the adsorbent bed porosity (between 0,25 and 0,37), so it is not a parameter of great interest.

It is also evident as a system that works with lower pressures performs better than one with higher pressures. At the same time, when the heat flux increases, it is possible to obtain a higher mass of fresh water but maximum temperatures reached by the system also increase. So, because of the available solar thermal energy depends on the location where the plant is installed, once the heat flux is fixed as a parameter, it can be easier to evaluate the best combination of the other physical quantities, always in order to obtain great performance. Moreover, because the evaporation temperature does not make a substantial contribution to the useful effects obtained, it is possible to set the process off also when the weather is cold. The limit of this model is that it works perfectly only with pressures not more higher than 1600 Pa, due to the hypothesis of the equations used. On the contrary, the adoption of solar energy is one of the the best options for the heat source in the AD systems.

This numerical and mathematical model, unfortunately, has not been experimentally-validated yet, but it will be as soon as the test bench will be implemented at the Polytechnic of Turin. In this perspective, many physical parameters, such as temperature or pressure that here have been hypothesised or calculated by several laws, will be measured by sensors, in order to refine, eventually, the model itself.

4.1 Future development

To investigate new and different geometries for the core or innovative bed materials, such as chemical adsorbents or composite ones, or moreover refrigerants different from water, can be other further possibilities, in order to optimize the performance of the system. In addition, the thermal model can be amplified, considering also the mass and heat transfer in the axial direction; so the height of the core can be considered as a parameter of interest. In conclusion, taking inspiration from Leong and Liu (2004), it may be attractive also to focus on the effect of the adsorbent particle diameter or the effect of the thickness of the adsorbent bed or, additionally, the effect of the silica gel regeneration temperature, and so on. It ought to be easy to do this, starting from the numerical model shown here and varying opportunely

the various parameters.

Chapter 5

Appendix

5.1 Variation of the Heat Flux at different pressures of the system

5.1.1 $T_{evap} = 20^{\circ}\text{C}$ and $P = 1100\text{ Pa}$

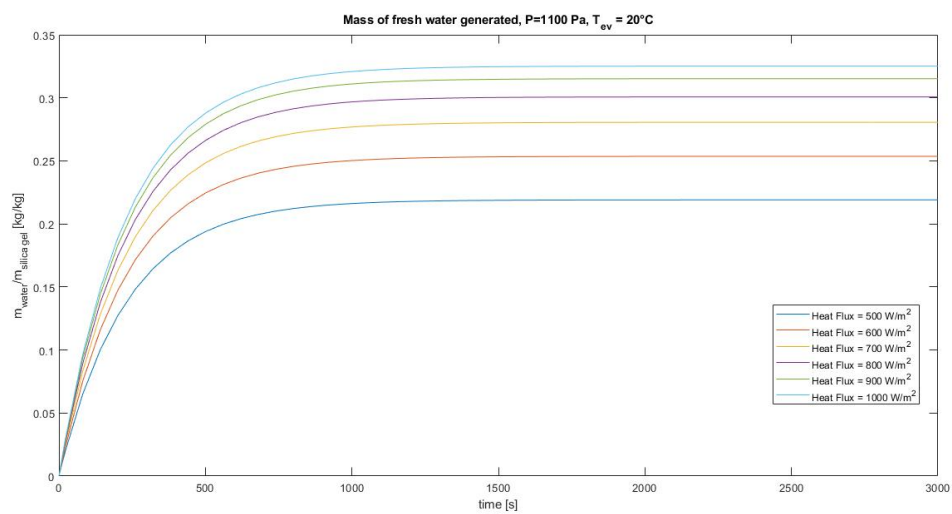


Figure 5.1: Mass of water generated in a single cycle from one bed, as a function of the Heat Flux, P=1100 Pa

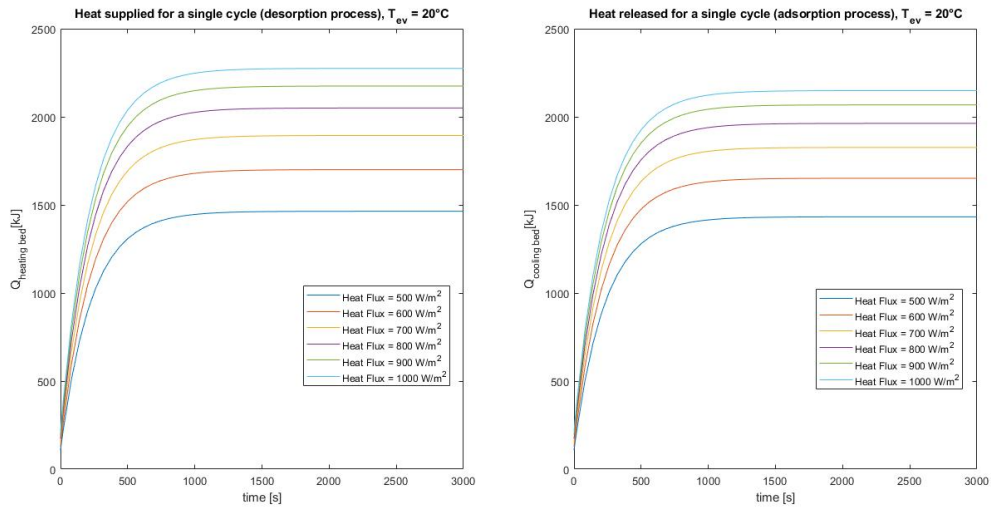


Figure 5.2: Total heating and cooling requirement of a single cycle, as a function of the Heat Flux, $P=1100$ Pa

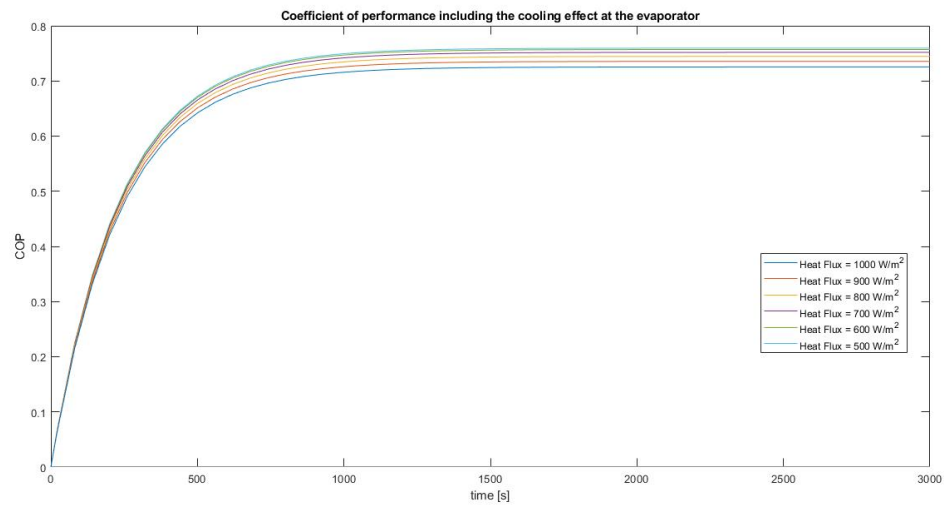


Figure 5.3: Coefficient of performance of the process, as a function of the Heat Flux, $P=1100$ Pa

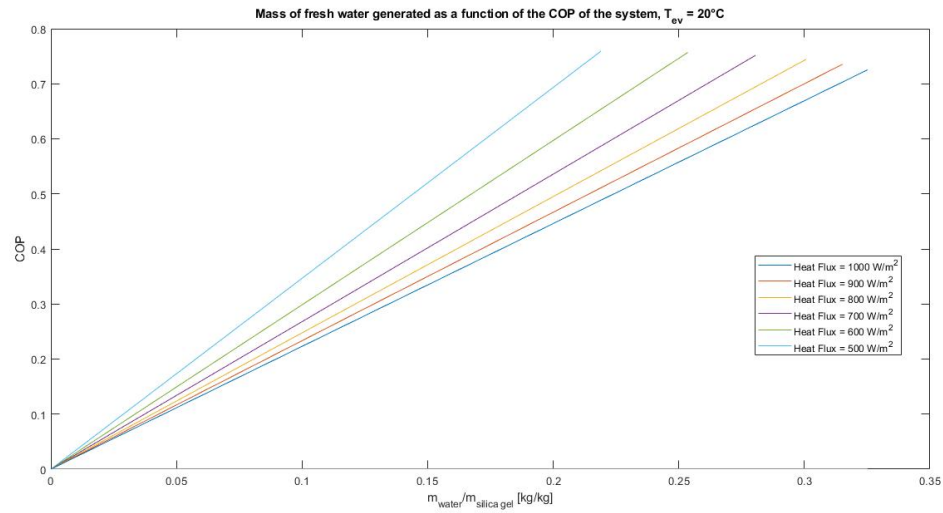


Figure 5.4: Coefficient of performance of the process as a function of the water production, $P=1100$ Pa

5.1.2 $T_{evap} = 20^\circ\text{C}$ and $P = 1200$ Pa

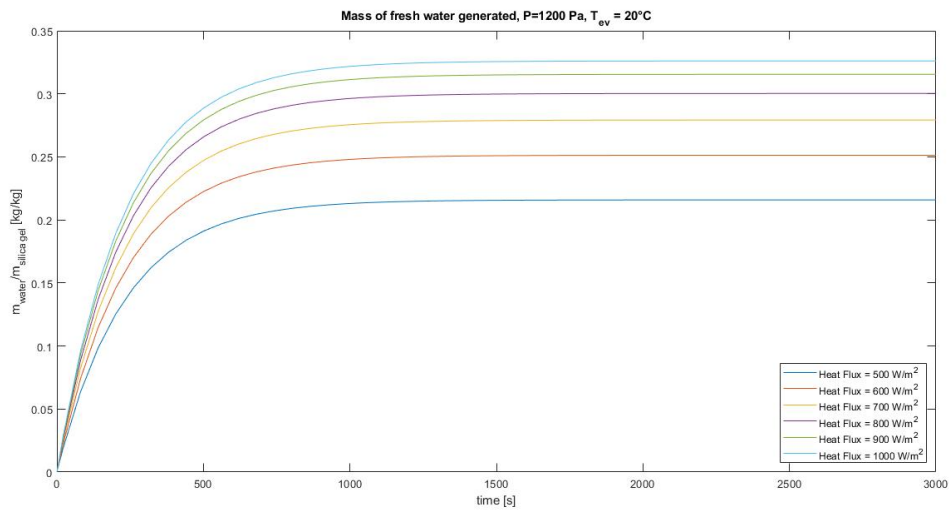


Figure 5.5: Mass of water generated in a single cycle from one bed, as a function of the Heat Flux, $P=1200$ Pa

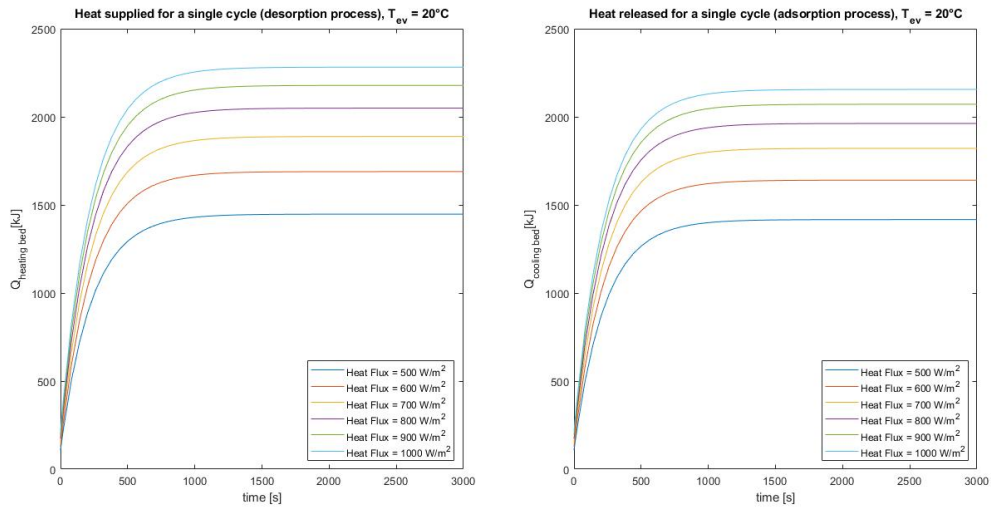


Figure 5.6: Total heating and cooling requirement of a single cycle, as a function of the Heat Flux, $P=1200$ Pa

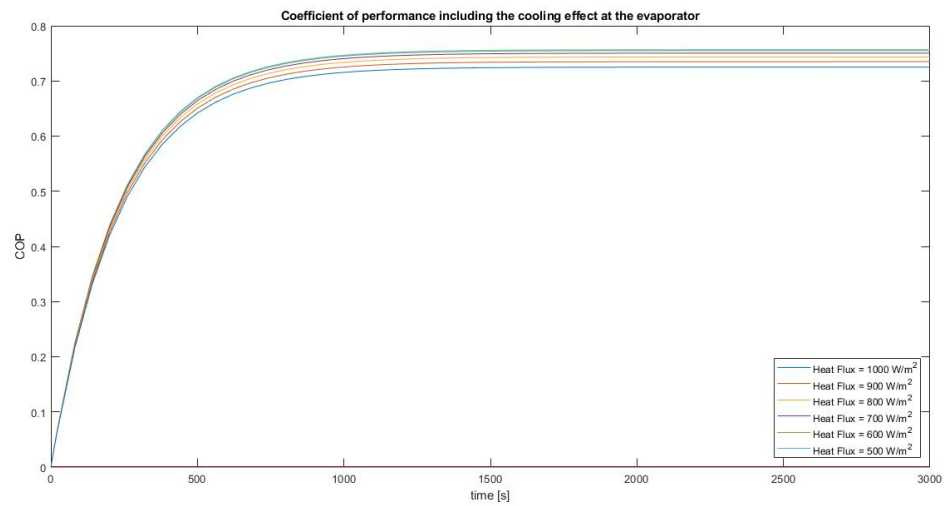


Figure 5.7: Coefficient of performance of the process, as a function of the Heat Flux, $P=1200$ Pa

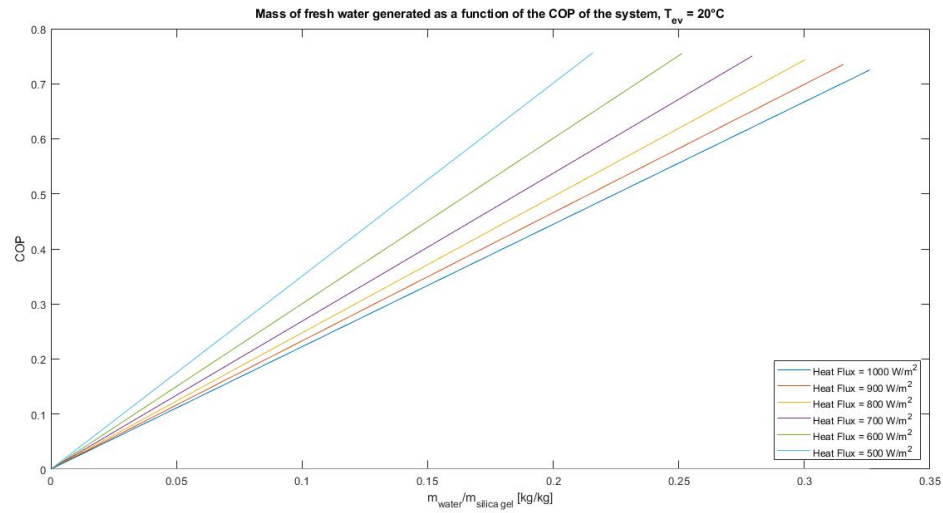


Figure 5.8: Coefficient of performance of the process as a function of the water production, $P=1200 \text{ Pa}$

5.1.3 $T_{evap} = 20^\circ\text{C}$ and $P = 1300 \text{ Pa}$

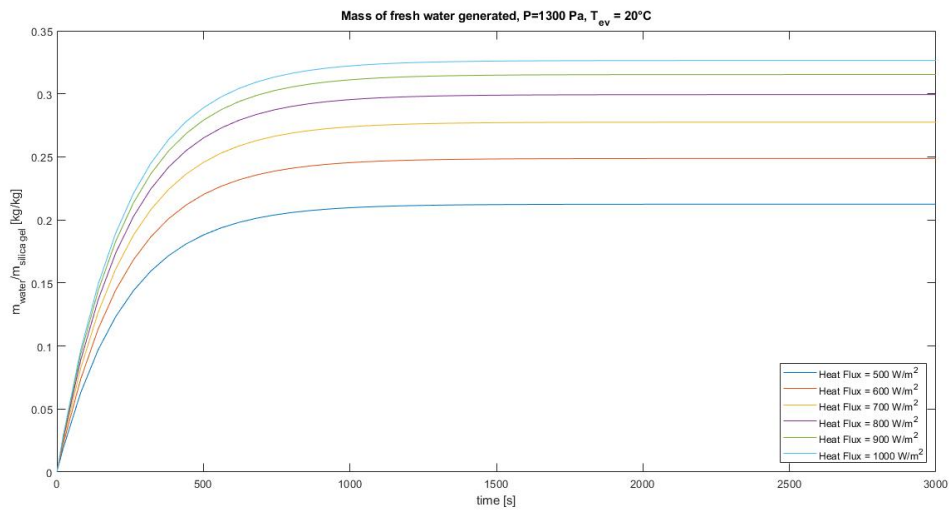


Figure 5.9: Mass of water generated in a single cycle from one bed, as a function of the Heat Flux, $P=1300 \text{ Pa}$

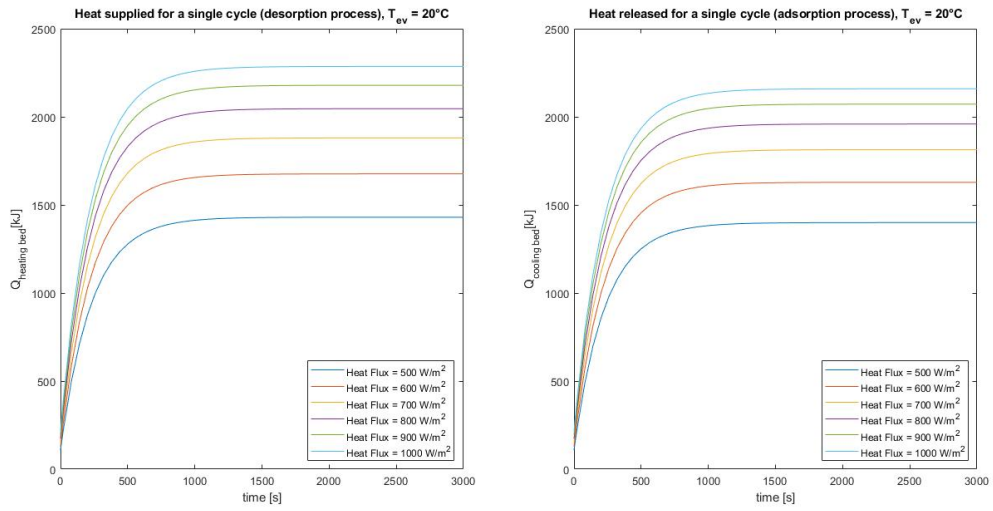


Figure 5.10: Total heating and cooling requirement of a single cycle, as a function of the Heat Flux, $P=1300$ Pa

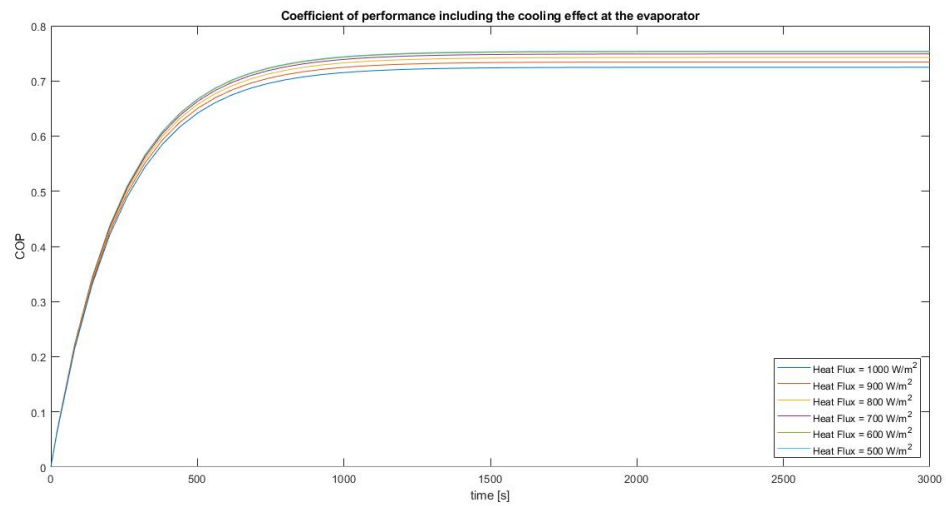


Figure 5.11: Coefficient of performance of the process, as a function of the Heat Flux, $P=1300$ Pa

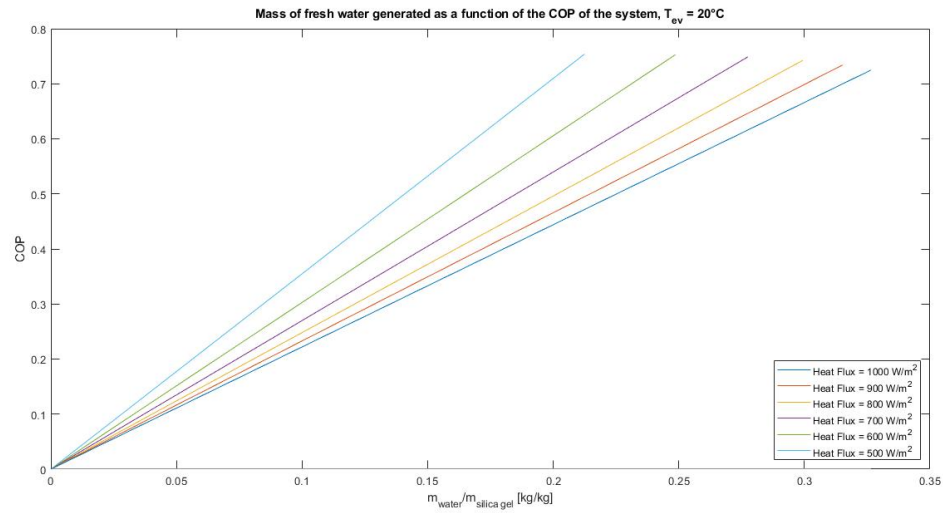


Figure 5.12: Coefficient of performance of the process as a function of the water production, $P=1300 \text{ Pa}$

5.1.4 $T_{evap} = 20^\circ\text{C}$ and $P = 1400 \text{ Pa}$

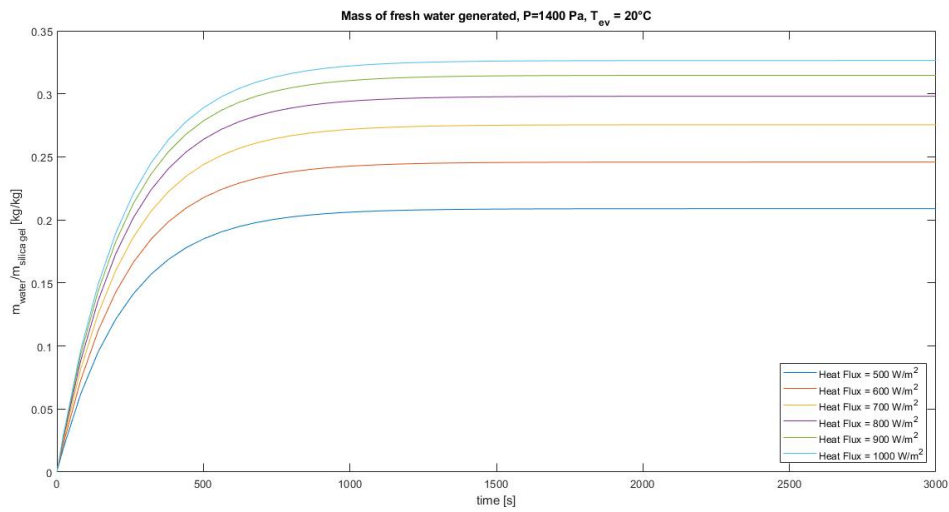


Figure 5.13: Mass of water generated in a single cycle from one bed, as a function of the Heat Flux, $P=1400 \text{ Pa}$

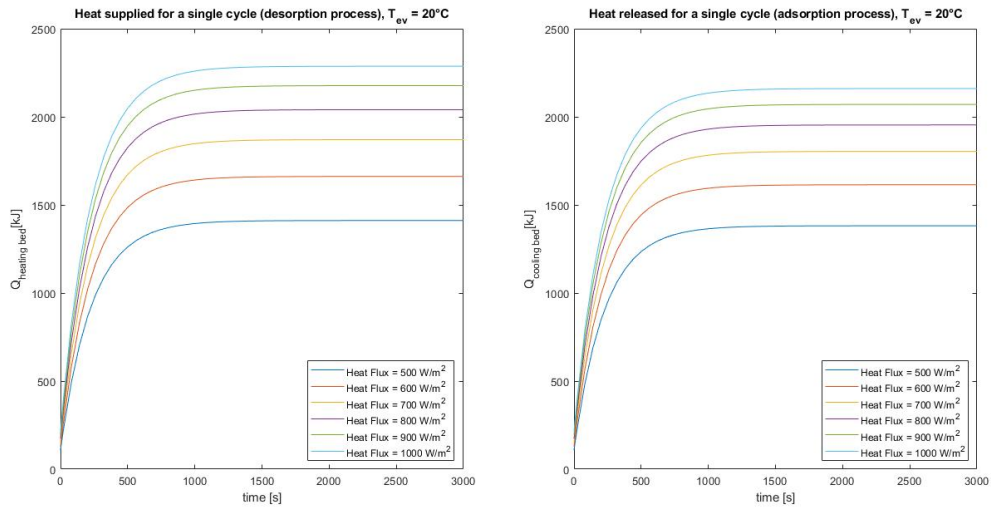


Figure 5.14: Total heating and cooling requirement of a single cycle, as a function of the Heat Flux, $P=1400$ Pa

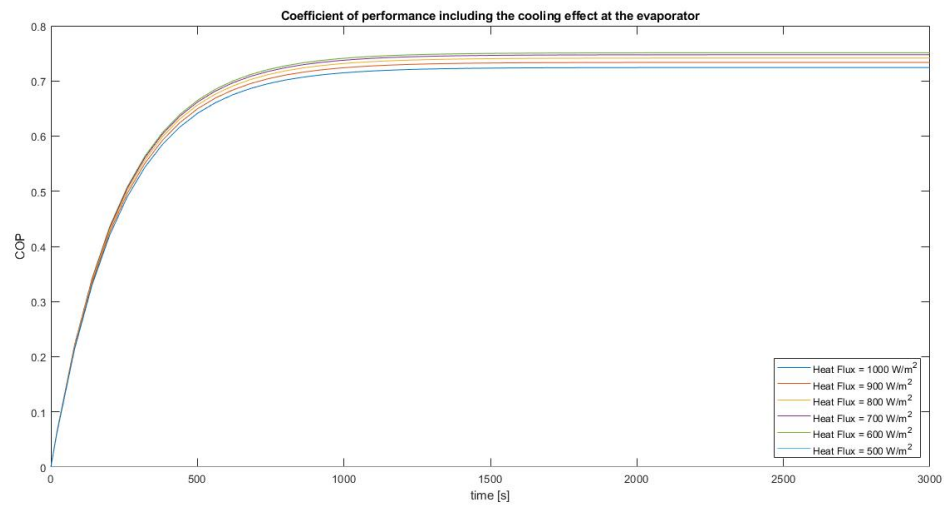


Figure 5.15: Coefficient of performance of the process, as a function of the Heat Flux, $P=1400$ Pa

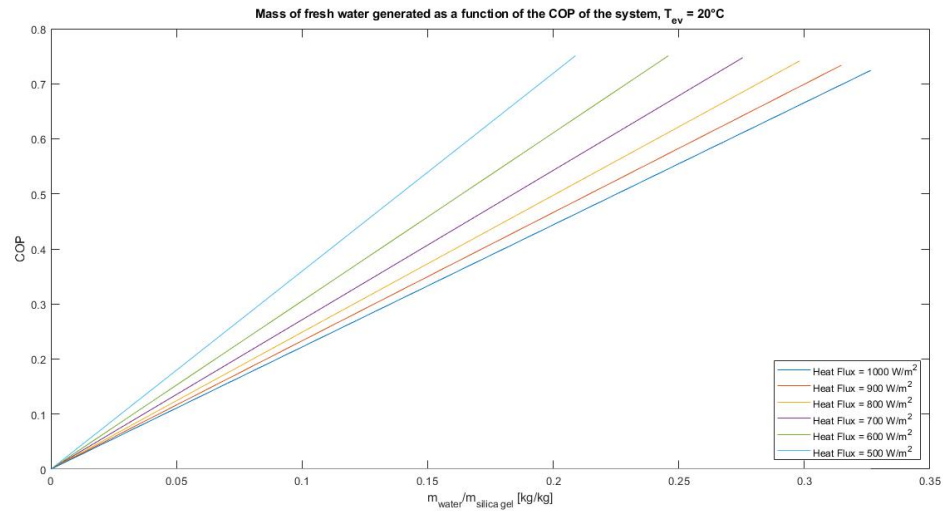


Figure 5.16: Coefficient of performance of the process as a function of the water production, $P=1400 \text{ Pa}$

5.2 Variation of the evaporation temperature at different pressures of the system

5.2.1 $\text{Heat Flux} = 500 \text{ W/m}^2$ and $P = 1100 \text{ Pa}$

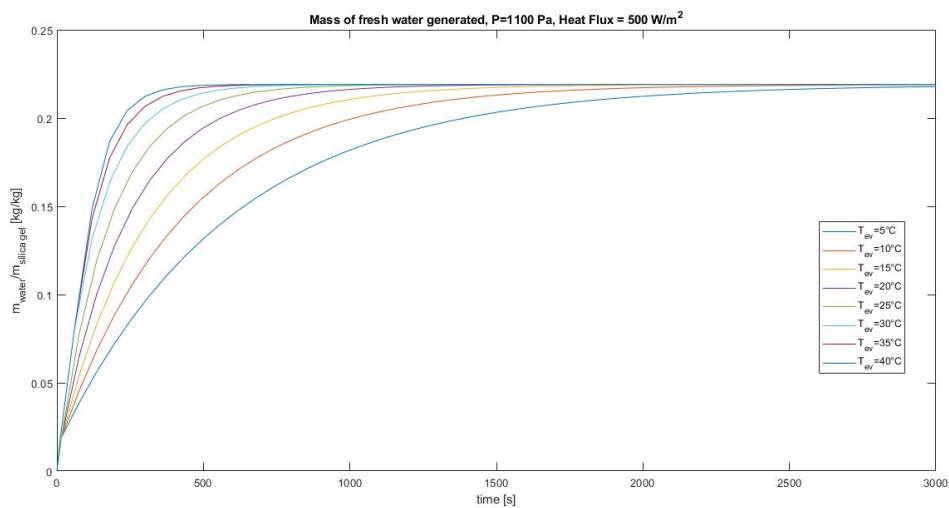


Figure 5.17: Mass of water generated in a single cycle from one bed, as a function of the evaporation temperature, $P=1100 \text{ Pa}$

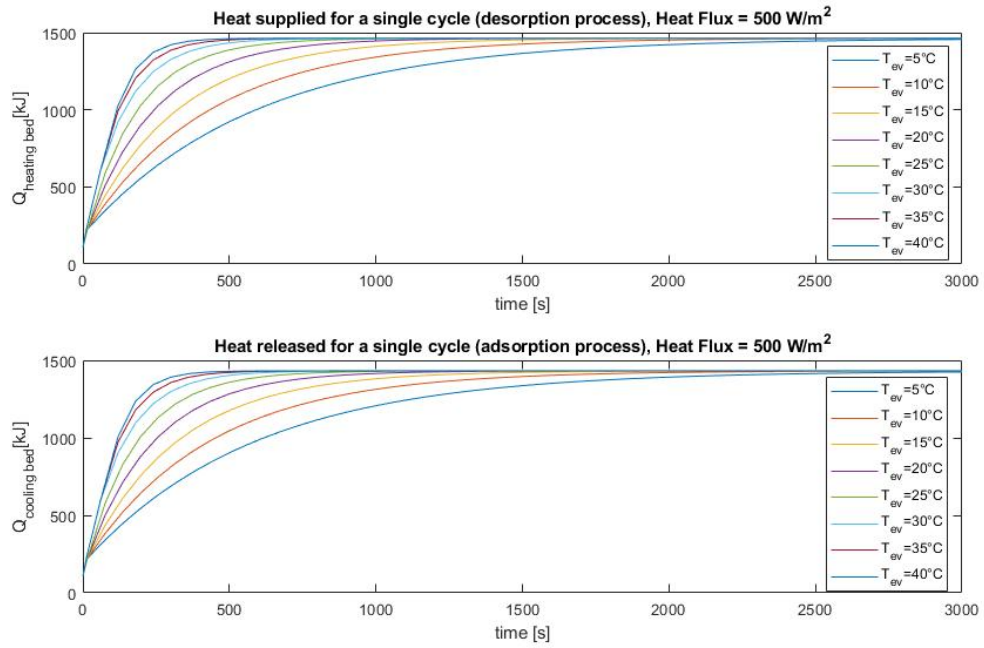


Figure 5.18: Total heating and cooling requirement of a single cycle, as a function of the evaporation temperature, $P=1100$ Pa

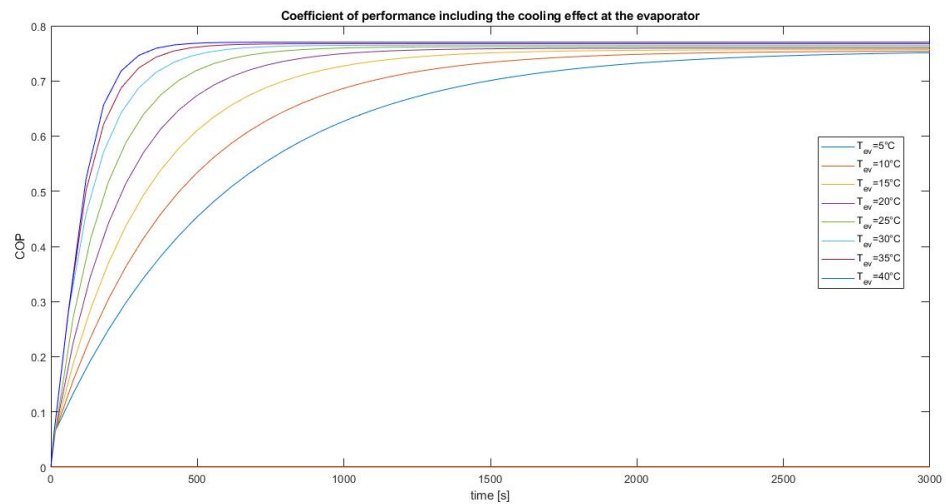


Figure 5.19: Coefficient of performance of the process, as a function of the evaporation temperature, $P=1100$ Pa

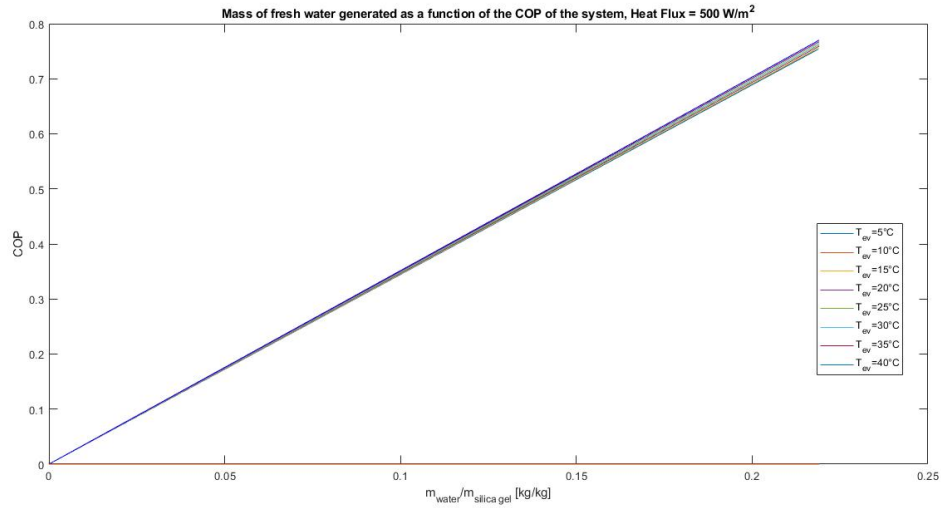


Figure 5.20: Coefficient of performance of the process as a function of the water production, $P=1100$ Pa

5.2.2 Heat Flux = 500 W/m^2 and $P = 1200$ Pa

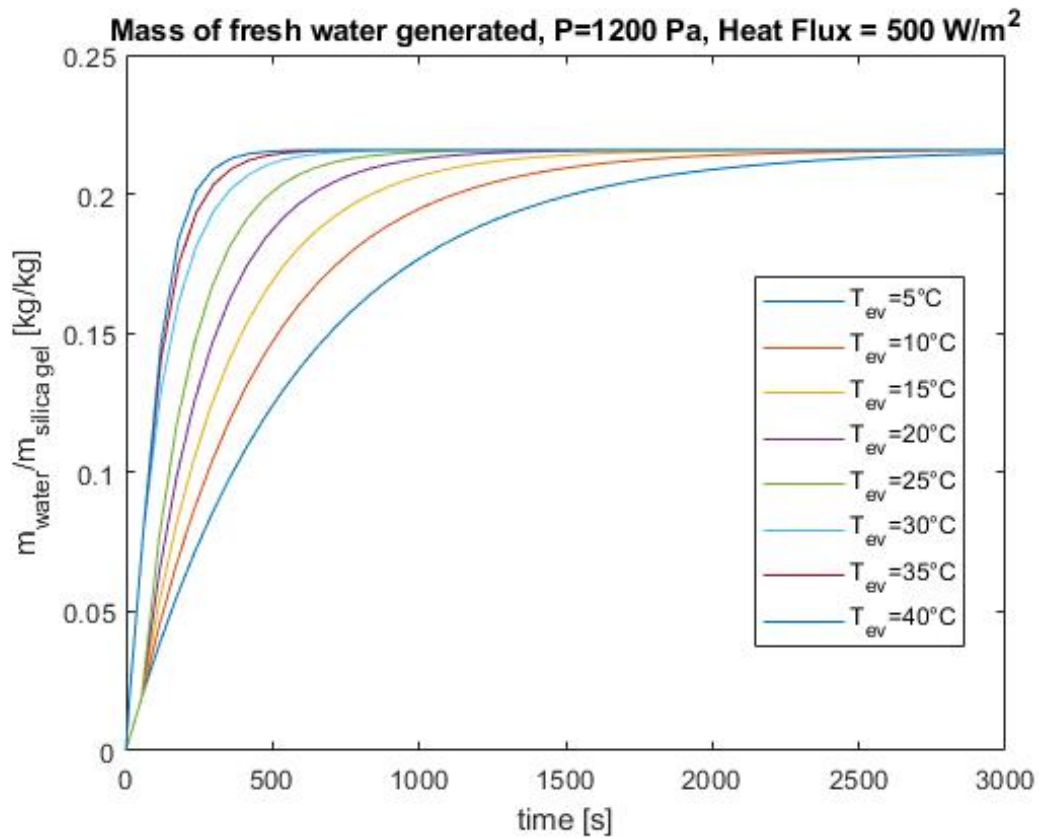


Figure 5.21: Mass of water generated in a single cycle from one bed, as a function of the evaporation temperature, $P=1200$ Pa

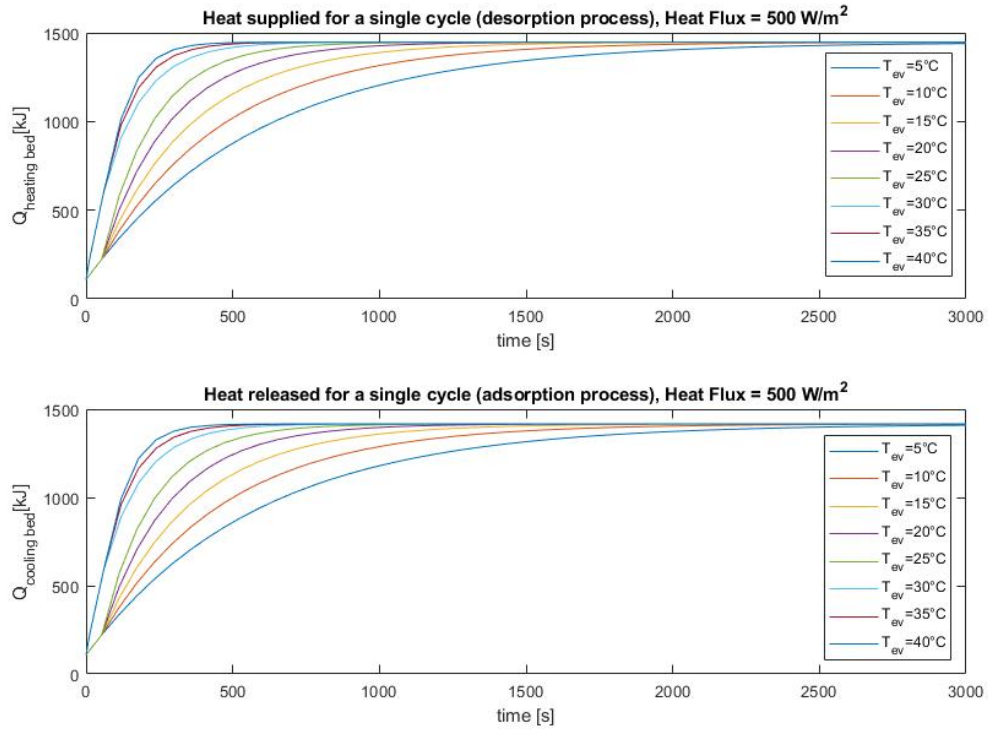


Figure 5.22: Total heating and cooling requirement of a single cycle, as a function of the evaporation temperature, P=1200 Pa

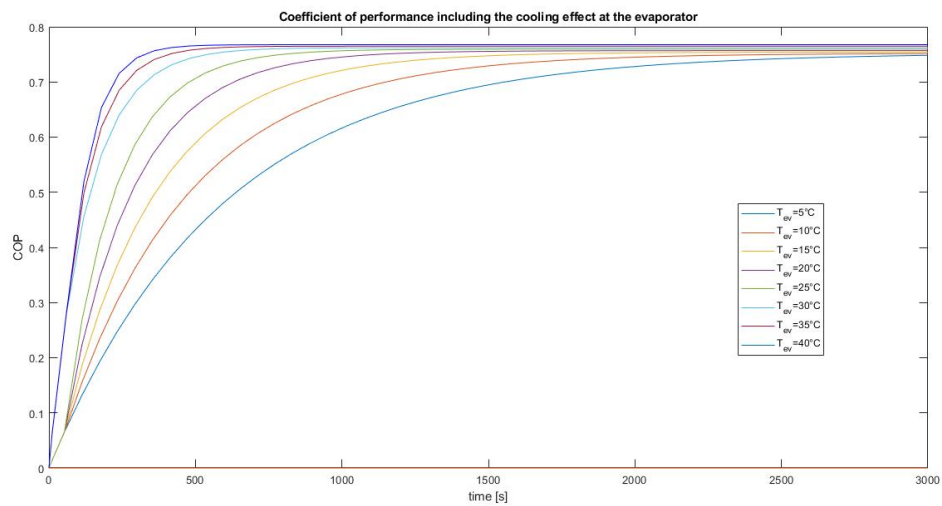


Figure 5.23: Coefficient of performance of the process, as a function of the evaporation temperature, P=1200 Pa

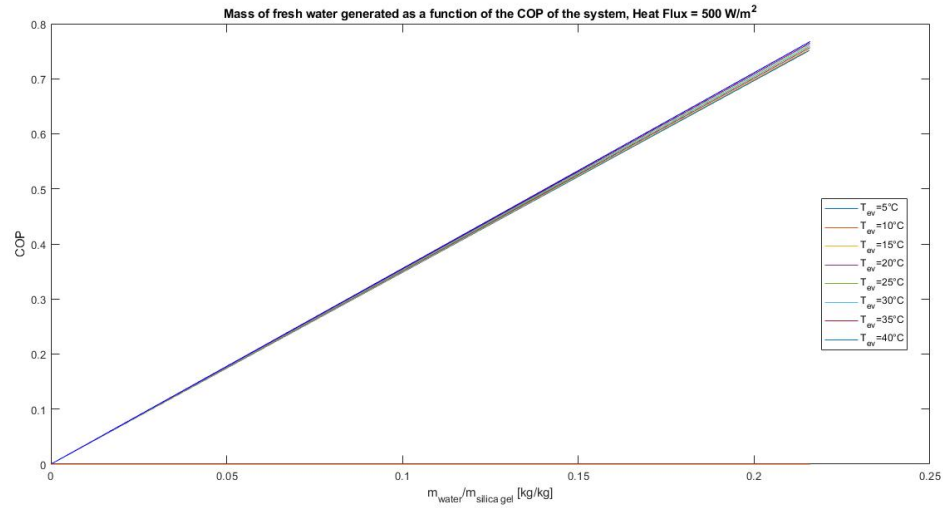


Figure 5.24: Coefficient of performance of the process as a function of the water production, $P=1200$ Pa

5.2.3 Heat Flux = 500 W/m^2 and $P = 1300$ Pa

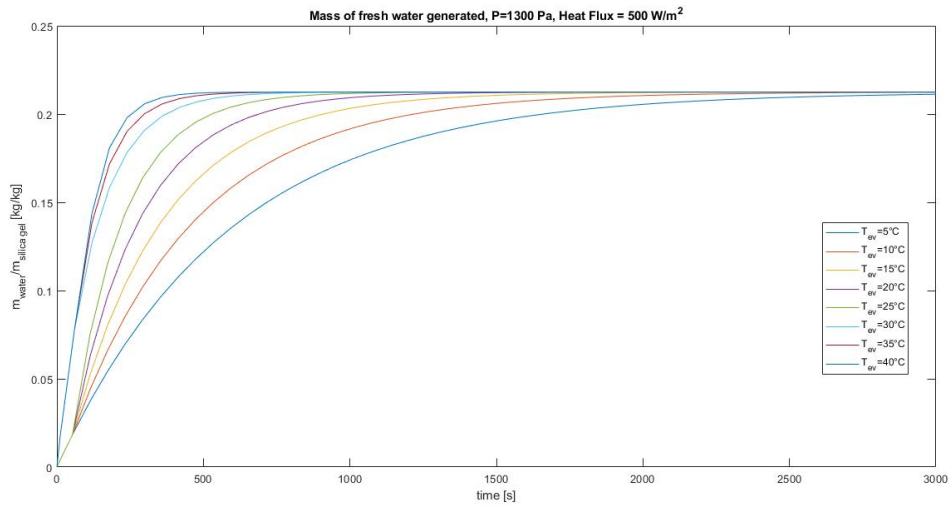


Figure 5.25: Mass of water generated in a single cycle from one bed, as a function of the evaporation temperature, $P=1300$ Pa

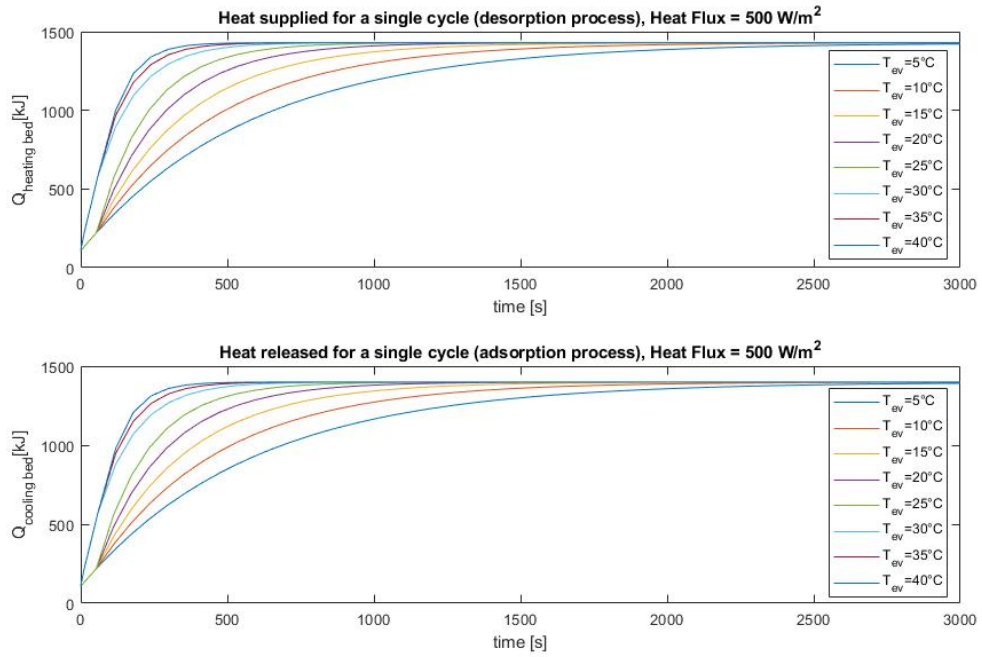


Figure 5.26: Total heating and cooling requirement of a single cycle, as a function of the evaporation temperature, P=1300 Pa

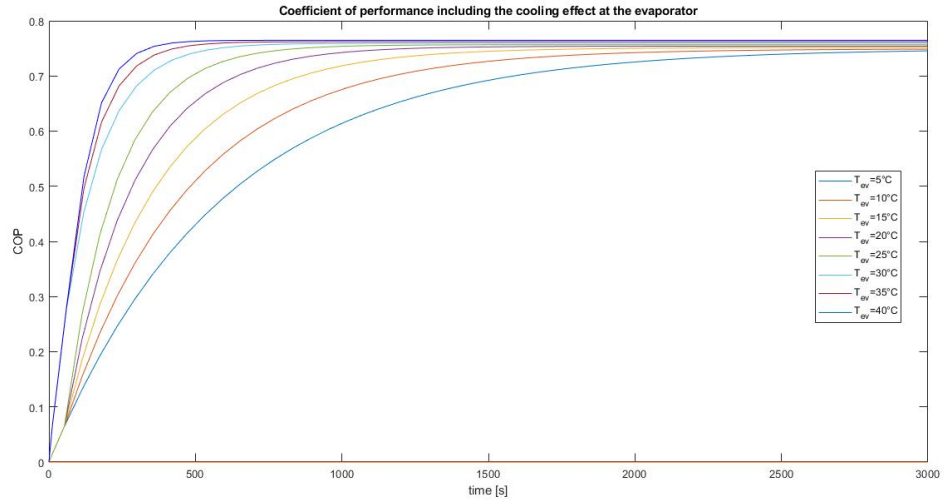


Figure 5.27: Coefficient of performance of the process, as a function of the evaporation temperature, P=1300 Pa

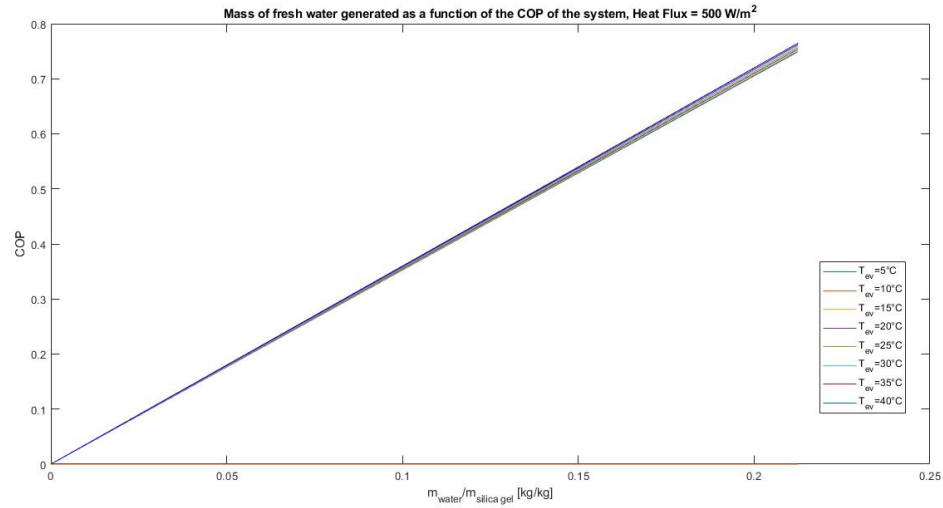


Figure 5.28: Coefficient of performance of the process as a function of the water production, $P=1300$ Pa

5.2.4 Heat Flux = 500 W/m^2 and $P = 1400$ Pa

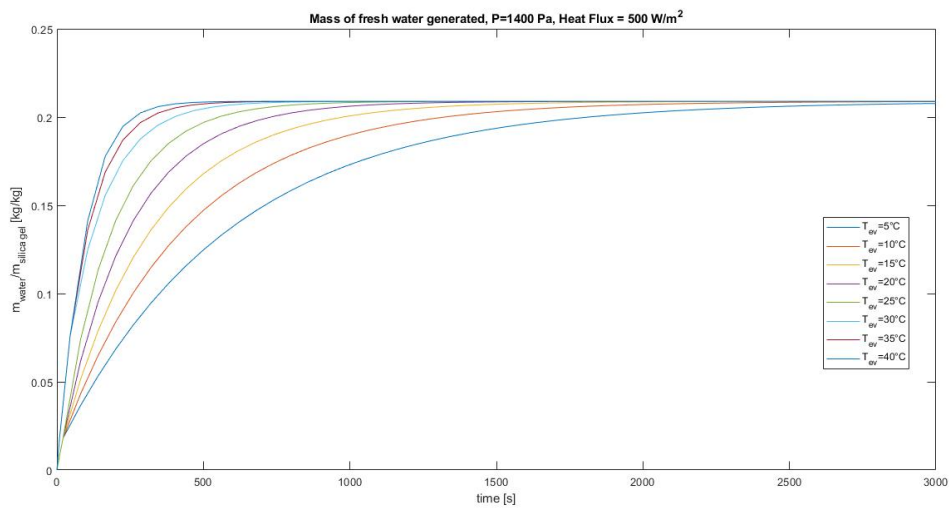


Figure 5.29: Mass of water generated in a single cycle from one bed, as a function of the evaporation temperature, $P=1400$ Pa

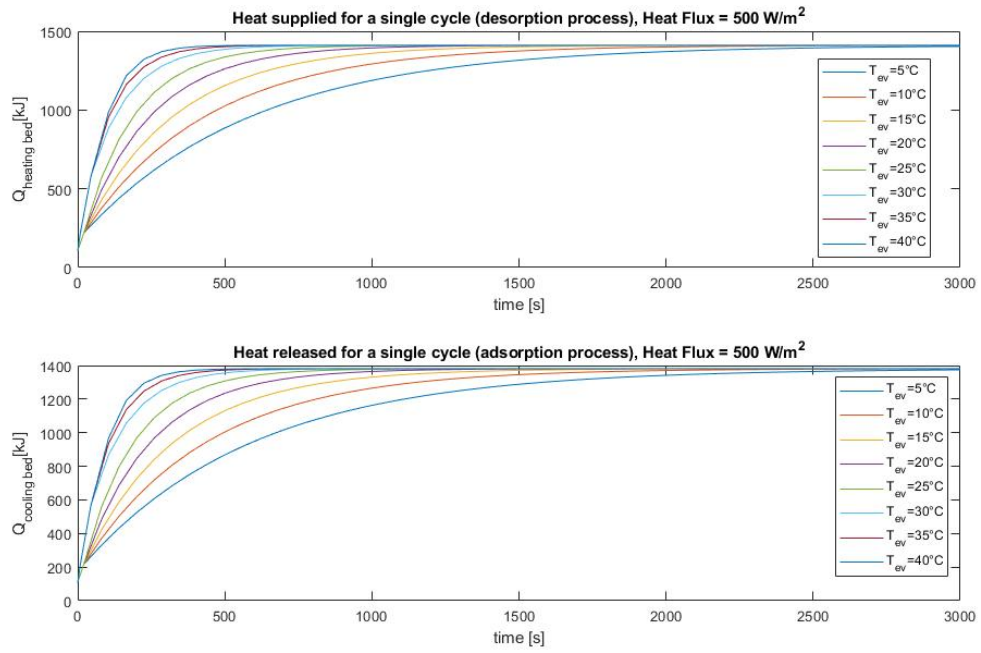


Figure 5.30: Total heating and cooling requirement of a single cycle, as a function of the evaporation temperature, $P=1400$ Pa

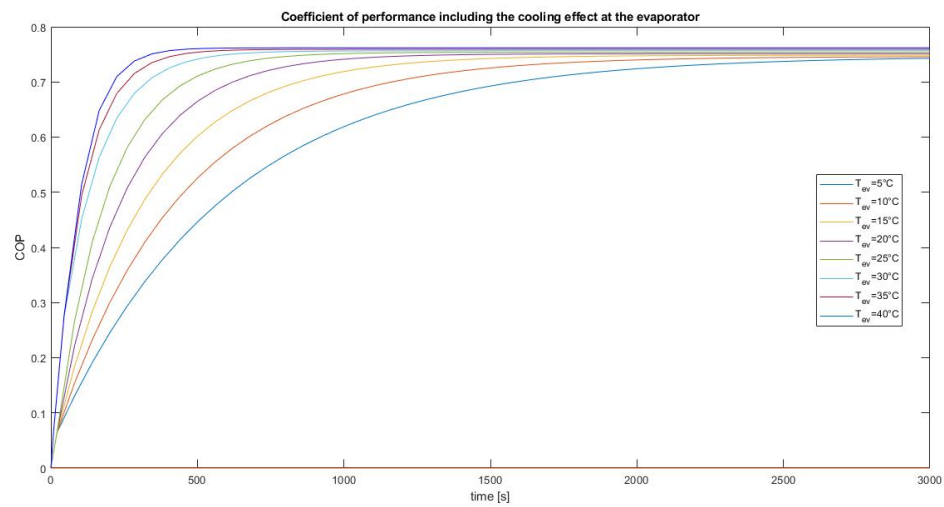


Figure 5.31: Coefficient of performance of the process, as a function of the evaporation temperature, $P=1400$ Pa

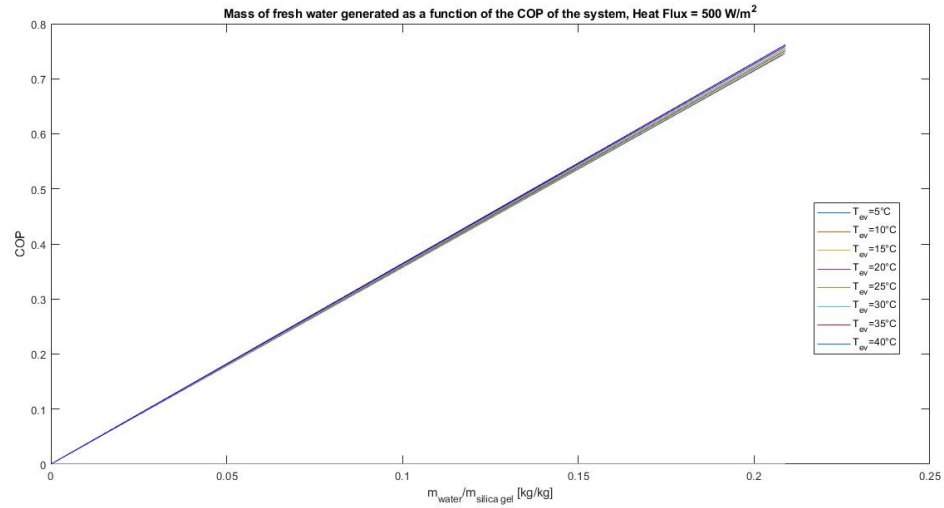


Figure 5.32: Coefficient of performance of the process as a function of the water production, $P=1400$ Pa

5.2.5 Heat Flux = 500 W/m² and $P = 1500$ Pa

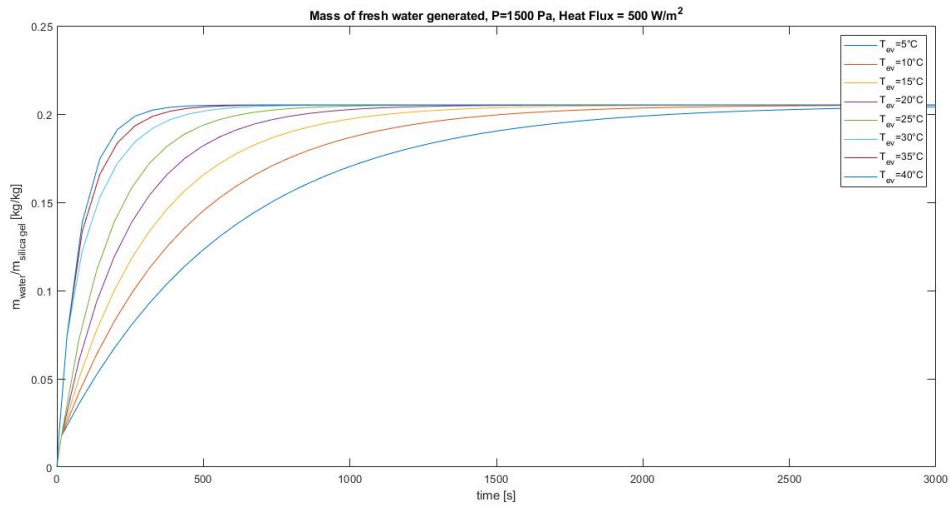


Figure 5.33: Mass of water generated in a single cycle from one bed, as a function of the evaporation temperature, $P=1500$ Pa

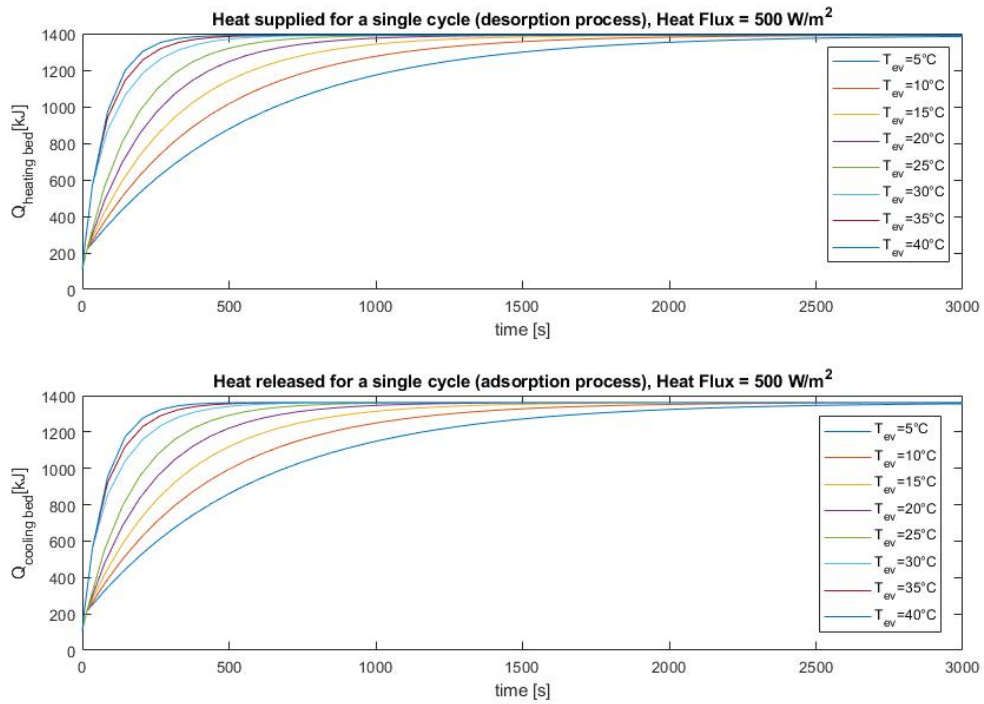


Figure 5.34: Total heating and cooling requirement of a single cycle, as a function of the evaporation temperature, $P=1500$ Pa

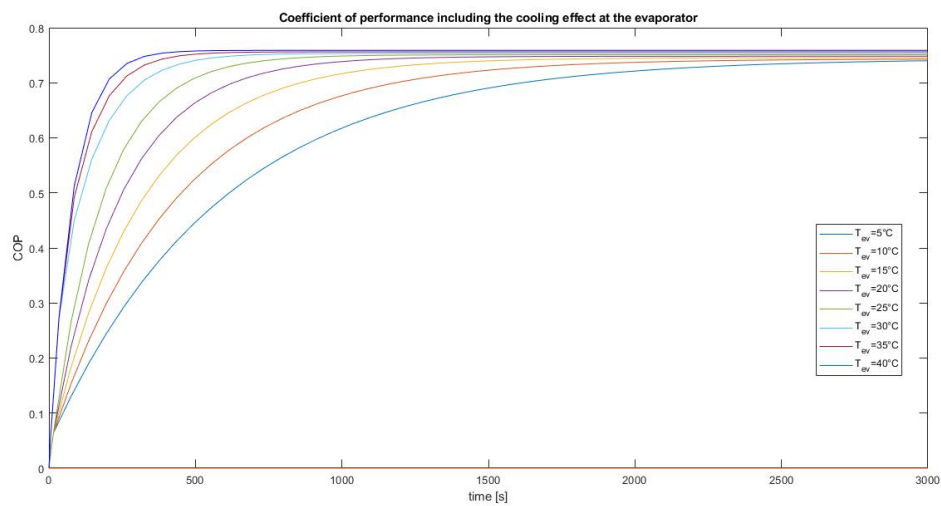


Figure 5.35: Coefficient of performance of the process, as a function of the evaporation temperature, $P=1500$ Pa

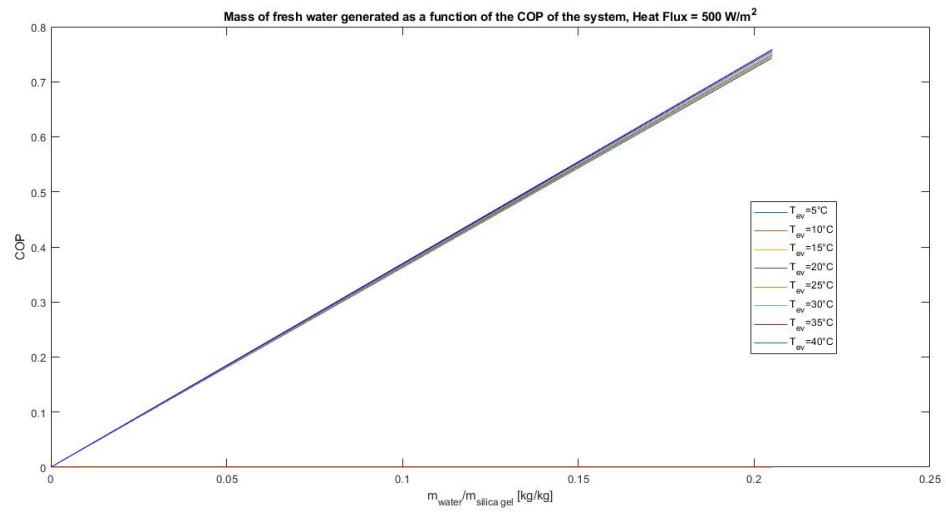


Figure 5.36: Coefficient of performance of the process as a function of the water production, $P=1500$ Pa

Acknowledgements

First of all my gratitude goes to my supervisors, Prof. Matteo Fasano, Prof. Eliodoro Chiavazzo and Dr. Matteo Morciano, for the skills and knowledge passed me down both during the university courses and the last months. Moreover, I thank them for giving me the chance to realize this project, for their help and full availability.

Secondly, my heartfelt thanks go to my family, for allowing me to get here, for putting up with me and for supporting me.

I am grateful to all those who never gave up on me and never made me feel in the wrong place.

Finally, I should like to express my particular thanks to the Polytechnic and the city of Turin, for making me grow up, personally and professionally, and live an unforgettable experience.

References

1. J.W. Wu, M.J. Biggs, E.J. Hu, Dynamic model for the optimisation of adsorption-based desalination processes, *Applied Thermal Engineering* 66 (2014) 464-473
2. A. Sakoda, M. Suzuki, Fundamental study on solar-powered adsorption cooling system, *J. Chem. Eng. Jpn.* 17 (1984) 52-57
3. A. Chakraborty, K. Thu, B.B. Saha, K.C. Ng, Adsorption-desalination cycle, *Advances in Water Desalination*, John Wiley & Sons, Inc., 2012, pp. 377-451
4. K.C. Ng, H.T. Chua, C.Y. Chung, C.H. Loke, T. Kashiwagi, A. Akisawa, B.B. Saha, Experimental investigation of the silica gel-water adsorption isotherm characteristics, *Appl. Therm. Eng.* 21 (2001) 1631-1642
5. K.C. Ng, K. Thu, A. Chakraborty, B.B. Saha, W.G. Chun, Solar-assisted dual-effect adsorption cycle for the production of cooling effect and potable water, *Int. J. Low Carbon Technol.* 4 (2) (2009) 61-67
6. K.C. Ng, K. Thu, Y. Kim, A. Chakraborty, G. Amy, Adsorption desalination: an emerging low-cost thermal desalination method, *Desalination* 308 (2013) 161-179
7. X. Wang, K.C. Ng, Experimental investigation of an adsorption desalination plant using low-temperature waste heat, *Appl. Therm. Eng.* 25 (2005) 2780-2789
8. X.L. Wang, H.T. Chua, Two bed silica gel-water adsorption chillers: an effectual lumped parameter model, *Int. J. Refrig.* 30 (2007) 1417-1426
9. L.W. Wang, R.Z. Wang, R.G. Oliveira, A review on adsorption working pairs for refrigeration, *Renewable and Sustainable Energy Reviews* 13 (2009) 518-534
10. J.W. Wu, M.J. Biggs, E.J. Hu, Thermodynamic analysis of an adsorption-based desalination cycle, *Chem. Eng. Res. Des.* 88 (2010) 1541-1547

11. K. Thu, A. Chakraborty, B.B. Saha, W.G. Chun, K.C. Ng, Life-cycle cost analysis of adsorption cycles for desalination, *Desalin. Water Treat.* 20 (2010) 1-10
12. K. Thu, B.B. Saha, A. Chakraborty, W.G. Chun, K.C. Ng, Study on an advance adsorption desalination cycle with evaporator-condenser heat recovery circuit, *Int. J. Heat Mass Transfer* 54 (2011) 43-51
13. K. Thu, A. Chakraborty, Y.D. Kim, A. Myat, B.B. Saha, K.C. Ng, Numerical simulation and performance investigation of an advanced adsorption desalination cycle, *Desalination* 308 (2013) 209-218
14. K.C. Ng, K. Thu, Y. Kim, A. Chakraborty, G. Amy, Adsorption desalination: an emerging low-cost thermal desalination method, *Desalination* 308 (2013) 161-179
15. Water desalination – Tap into the liquid Gold, Leonard Wagner, December 2007
16. A. Li, A.B. Ismail, K. Thu, K.C. Ng, W.S. Loh, Performance evaluation of a zeolite–water adsorption chiller with entropy analysis of thermodynamic insight, *Applied Energy* 130 (2014) 702–711
17. K.C. Leong, Y. Liu, Numerical modeling of combined heat and mass transfer in the adsorbent bed of a zeolite/water cooling system, *Applied Thermal Engineering* 24 (2004) 2359–2374
18. R. Raj, V. Baiju, Thermodynamic Analysis of a Solar Powered Adsorption Cooling and Desalination System, *Energy Procedia* 158 (2019) 885-891
19. A. Sakoda, M. Suzuki, Simultaneous transport of heat and adsorbate in closed type adsorption cooling system utilizing solar heat, *Journal of Solar Energy Engineering*, (1986) Vol. 108-239
20. D. Zejli, R. Benchrifa, A. Bennouna, O.K. Bouhelal, A solar adsorption desalination device: first simulation results, *Desalination* 168 (2004) 127-135
21. H.T. Chua, K.C. Ng, C.Y. Chung, A. Malek, T. Kashiwagi, A. Akisawa, B.B. Saha, Modeling the performance of two-bed, silica gel-water adsorption chillers, *Int. J. Refrig.* 22 (1999) 194-204

22. H.T. Chua, K.C. Ng, W. Wang, C. Yap, X.L. Wang, Transient modelling of a two bed silica gel-water adsorption chiller, *Int. J. Heat Mass Transfer* 47 (2004) 659-669
23. R.A. Rouf, K.C.A. Alam, M.A.H. Khan, B.B. Saha, F. Meunier, M.A. Alim, K.M.A. Kabir, Advancement of solar adsorption cooling by means of heat storage, *Procedia Engineering* 90 (2014) 649-656
24. D.C. Wang, Z.Z. Xia, J.Y. Wu, R.Z. Wang, H. Zhai, W.D. Dou, Study of a novel silica gel-water adsorption chiller. Part I. Design and performance prediction, *Int. J. Refrig.* 28 (2005) 1073-1083
25. A.S. Ulku, M. Mobedi, Adsorption in energy storage, *Energy Storage Systems*. 487-507
26. A.O. Dieng, R.Z. Wang, Literature review on solar adsorption technologies for ice-making and air conditioning purposes and recent developments in solar technology, *Renewable and Sustainable Energy Reviews* 5 (2001) 313-342
27. Y. Liu, K.C. Leong, The effect of operating conditions on the performance of zeolite/water adsorption cooling systems, *Applied Thermal Engineering* 25 (2005) 1403-1418
28. Y.L. Zhao, E. Hu, A. Blazewicz, A non-uniform pressure and transient boundary condition based dynamic modeling of the adsorption process of an adsorption refrigeration tube, *Appl. Energy* 90 (2011) 280-287
29. G. Zhang, D.C. Wang, J.P. Zhang, Y.P. Han, W. Sun, Simulation of operating characteristics of the silica gel-water adsorption chiller powered by solar energy, *Solar Energy* 85 (2011) 1469-1478
30. H. Deshmukh et al., Study of sorption based energy storage system with silica gel for heating application, *Appl. Therm. Eng.* (2016)
31. Ghaffour N. et al. Renewable energy-driven innovative energy-efficient desalination technologies. *Appl Energy* (2014)
32. S. Mitra, K. Srinivasan, P. Kumar, S.S. Murthy, P. Dutta, Solar driven Adsorption Desalination system, *Energy Procedia* 49 (2014) 2261 – 2269

33. A. Myat, K.C. Ng, K. Thu, Y. Kim, Experimental investigation on the optimal performance of zeolite-water adsorption chiller, *Appl. Energy* 2013 (2013) 582-590
34. G. Maggio, A. Freni, G. Restuccia, A dynamic model of heat and mass transfer in a double-bed adsorption machine with internal heat recovery, *International Journal of Refrigeration* 29 (2006) 589–600
35. G. Najeh, G. Slimane, M. Souad, B. Riad, E.G. Mohammed, Performance of silica gel-water solar adsorption cooling system, *Case Studies in Thermal Engineering* (2016)
36. G. Najeh, S. Gabsi, E.G. Mohammed, B. Riad, Experimental Analysis of a Solar Adsorption System Refrigeration Cycle with Silica-Gel/Water Pair, *Journal of Fundamentals of Renewable Energy and Applications* (2021), Vol.11 No.1
37. Chapter Four - Membrane Distillation, Vassilis Belessiotis, Soteris Kalogirou, Emmy Delyannis, *Thermal Solar Desalination, Methods and Systems*, 2016, Pages 191-
38. Desalination by Freeze Crystallization: An Overview, Khadije El Kadi, Isam Janajreh, *Int. J. of Thermal & Environmental Engineering*, Volume 15, No. 2 (2017) 103-110
39. Hesamoddin Rabiee, Kaveh RajabKhalilpour, John M. Betts, Nigel Tapper, Chapter 13 - Energy-Water Nexus: Renewable-Integrated Hybridized Desalination System, *Polygeneration with Polystorage for Chemical and Energy Hubs For Energy and Chemicals*, 2019, Pages 409-458
40. Salah Ud-Din Khan, Shahab Ud-Din Khan, Syed Noman Danish, Jamel Orfi, Usman Ali Rana, Sajjad Haide, Chapter 6 - Nuclear Energy Powered Seawater Desalination, *Renewable Energy Powered Desalination Handbook Application and Thermodynamics*, 2018, Pages 225-264
41. E. Kondili, *Special Wind Power Applications*, *Earth Systems and Environmental Sciences Comprehensive Renewable Energy*, Volume 2, 2012, Pages 725-746
42. S.C. Bhatia, *Cogeneration*, *Advanced Renewable Energy Systems*, 2014

43. Ibrahim Dincer, Marc A. Rosen, Cogeneration, Multigeneration and Integrated Energy Systems, in Exergy Analysis of Heating, Refrigerating and Air Conditioning, 2015
44. IWMI report, Insights from the Comprehensive Assessment of Water Management in Agriculture, Stockholm World Water Week, 2006
45. <https://smartwatermagazine.com/q-a/what-meaning-desalination>
46. <https://www.bryair.com/news-and-events/articles/what-is-silica-gel-and-what-are-the-advantages-of-it-as-a-desiccant/>
47. <https://www.britannica.com/science/multistage-flash-distillation>
48. <https://www.britannica.com/science/multiple-effect-distillation>
49. R. Bubbico, B. Mazzarotta, C. Menale (Università di Roma “Sapienza”), Confronto tramite test sperimentali e simulazione numerica di diverse soluzioni per migliorare le prestazioni dell’accumulo termico, ENEA, Settembre 2016